preparation of perovskite powders via a vibro-milling technique [12–14], to our knowledge a detailed study considering the role of both milling times and firing conditions on the preparation of perovskite nanopowders has not been widely reported yet.

In the present study, we have demonstrated the potential of a rapid vibro-milling technique in the production of several important perovskite nanopowders, such as PbZrO₃ or PZ, PbTiO₃ or PT and BaTiO₃ or BT.

2. Experimental

The raw materials used were commercially available lead oxide, zirconium oxide, titanium oxide and barium carbonate (Fluka, >99% purity). These oxide powders exhibited an average particle size in the range of 3.0–5.0 μm. PbZrO₃, PbTiO₃ and BaTiO₃ powders were synthesized by the solid-state reaction of these raw materials. A vibratory laboratory mill (McCrone Micronizing Mill) powered by a 1/30 HP motor was employed for preparing the stoichiometric powders [13]. The grinding vessel consists of a 125 ml capacity polypropylene jar fitted with a screw-capped, gasketless, polythene closure. The jar is packed with an ordered array of identical, cylindrical, grinding media of polycrystalline corundum. A total of 48 milling media cylindrical with a powder weight of 20 g was kept constant in each batch. The milling operation was carried out in isopropanal inert to the polypropylene jar. Various milling times ranging from 0.5 to 35 h were selected in order to investigate the phase formation characteristic of all desired powders and the smallest particle size. After drying at 120 °C for 2 h, various calcination conditions, i.e. temperature ranging from 500 to 1200 °C, dwell times ranging from 1 to 6 h and heating/cooling rates ranging from 10 to 30 °C/min, were applied (the powders were calcined inside a closed alumina crucible) in order to investigate the formation of the desired phases.

All powders were examined by room temperature X-ray diffraction (XRD; Siemens-D500 diffractometer) using Ni-filtered Cu K α radiation, to identify the phases formed, optimum milling time and firing conditions for the production of single-phase powders. The average crystallite size is also estimated from XRD patterns [15]. The particle size distributions of the powders were determined by laser diffraction technique (DIAS 1640 laser diffraction spectrometer) with the particle sizes and morphologies of the powders observed by scanning electron microscopy (JEOL JSM-840A SEM). The chemical compositions of the phases formed were elucidated by an energy-dispersive X-ray (EDX) analyzer with an ultra-thin window. EDX spectra were quantified with the virtual standard peaks supplied with the Oxford Instruments eXL software.

3. Results and discussion

XRD patterns of the calcined PbZrO₃ powders after different combination of milling time and calcination condition are given

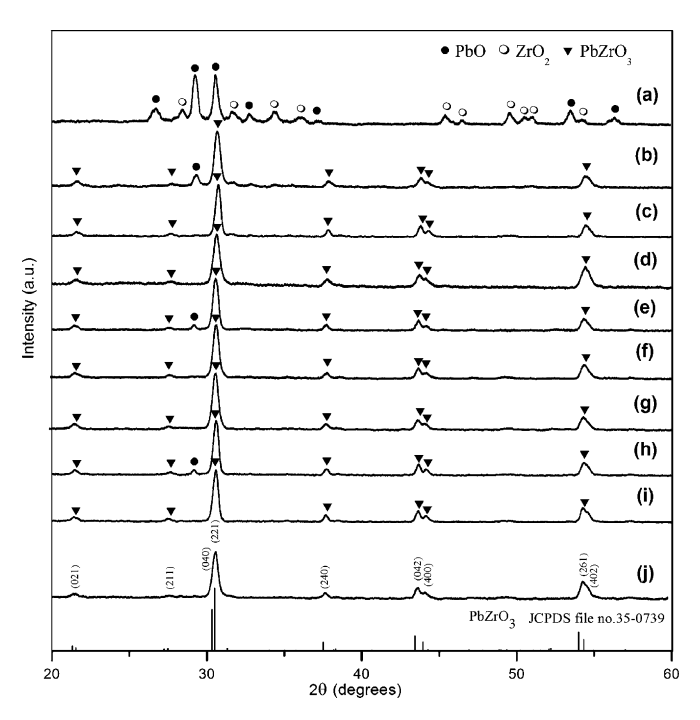


Fig. 1. XRD patterns of PZ powders milled for 15 h (a) uncalcined, and calcined at 800 °C for (b) 1 h and (c) 2 h with heating/cooling rates of 10 °C/min and (d) 30 °C/min; milled for 25 h and calcined at (e) 750 °C for 5 h (f) 800 °C for 1 h with heating/cooling rates of 10 °C/min and (g) 30 °C/min.; and milled for 35 h and calcined at 750 °C for (h) 3 h and (i) 4 h with heating/cooling rates of 10 °C/min and (j) 30 °C/min.

in Fig. 1. For the uncalcined powder subjected to 15 h of vibro-milling, only X-ray peaks of precursors PbO (●) and ZrO₂ (○) are present, indicating that no reaction was yet triggered during the vibro-milling process. However, after calcination at 800 °C for 1 h, it is seen that the perovskite PbZrO₃ becomes the predominant phase, indicating that the reaction has occurred to a considerable extent. It should be noted that when the dwell time of the calcination at 800 °C was extended up to 2 h, the single-phase of perovskite PZ (yield of 100% within the limitations of the XRD technique) was obtained. This was apparently a consequence of the enhancement in crystallinity of the perovskite phase with increasing degree of mixing and dwell time, in good

Table 1 Effect of milling time on the variation of particle size of perovskite powders calcined at their optimum conditions with heating/cooling rates of 30 °C/min and measured by different techniques

Powders	Milling time (h)	Calcination condition (°C/h)	XRD A (nm)	SEM		Laser scattering	
				D (nm)	P (nm)	$\overline{D \text{ (nm)}}$	P (nm)
PZ	15	800/2	60.41	280	53–692	700	35–2000
	25	800/1	35.11	223	31-400	170	35-750
	35	750/4	27.50	121	31–228	1570	10-6000
PT	5	600/1	22.50	101	67–135	690	290-1140
	15	600/1	22.00	78	43-114	4640	1640-7790
	25	600/1	21.50	63	17–109	180	70–310
BT	0.5	1300/2	38.32	610	250-1400	1000	400-1500
	25	1200/2	31.60	390	250-700	400	60-700
	30	1200/2	31.56	250	100-400	600	120-1000

A: Crystallite size; D: average particle size; P: particle size distribution or range.

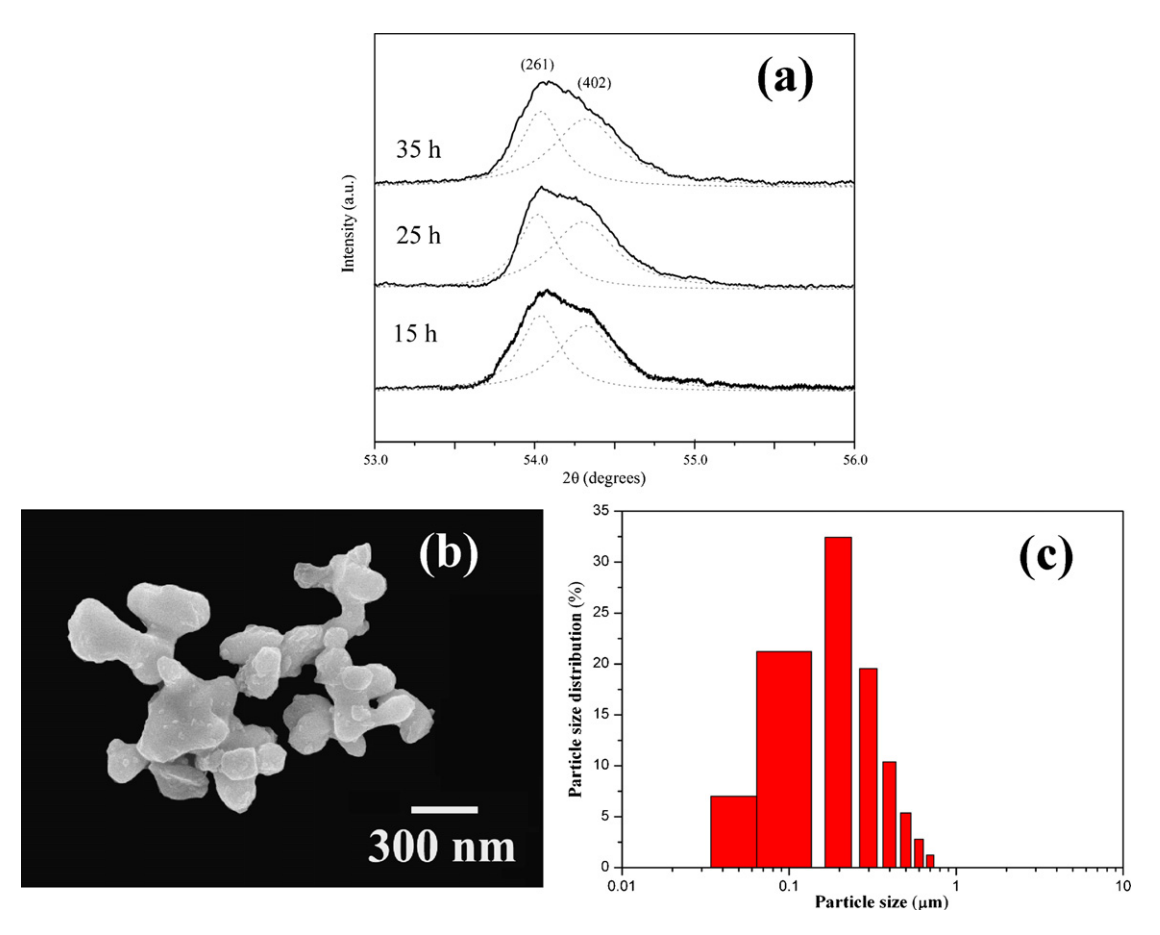


Fig. 2. (a) Enlarged zone of XRD patterns showing peaks broadening as a function of milling times of PZ powders, (b) SEM micrograph and (c) particle size distribution of PZ powders milled for 25 h and calcined at 800 °C for 1 h with heating/cooling rates of 30 °C/min.

agreement with other works [13,14]. In general, the strongest reflections apparent in the majority of these XRD patterns indicate the formation of the lead zirconate, PbZrO₃. These can be matched with JCPDS file number 35-0739 for the orthorhombic phase, in space group P2cb (no. 32) with cell parameters a=823 pm, b=1177 pm and c=588 pm [16], consistent with other works [17,18]. For 15 h of milling, the optimum calcination condition for the formation of a high purity PbZrO₃ phase was found to be about $800\,^{\circ}$ C for 2 h with heating/cooling rates of $30\,^{\circ}$ C/min.

To further study the phase development with increasing milling times, an attempt was also made to calcine mixed powders milled at 25 and 35 h under various conditions as shown in Fig. 1(e–j). In this connection, it is seen that by varying the calcination condition, the minimum firing temperature for the single-phase formation of each milling batch is gradually decreased with increasing milling time. The main reason for this behavior is that a complete solid-state reaction probably takes place more easily when the particle size is milled down by accelerating an atomic diffusion mechanism to meet the suitable level of homogeneity mixing. It is thought that reducing the particle size significantly reduces heat diffusion limitations. It is therefore, believed that the solid-state reaction to form perovskite PZ phase occurs at lower temperatures with decreasing the particle size of the oxide powders.

In the work reported here, evidence for the minor phase of PbO which coexists with the parent phase of PbZrO₃ is found after calcination at temperature 750–800 °C, in agreement with literature [11,19]. This second phase has an orthorhombic structure with cell parameters a = 589.3 pm, b = 549.0 pm and c = 475.2 pm (JCPDS file number 77-1971) [20]. This observation could be attributed mainly to the poor reactivity of lead and zirconium species [19] and also the limited mixing capability of the mechanical method [13,14]. A noticeable difference is noted when employing the milling time longer than 15 h, Fig. 1(e-j), since an essentially monophasic PbZrO₃ of perovskite structure was obtained at 800 °C for 1 h (or 750 °C for 4 h) for the milling time of 25 h (or 35 h). This was apparently a consequence of the enhancement in crystallinity of the perovskite phase with increasing degree of mixing and dwell time, in good agreement with other works [13,14].

In the present study, an attempt was also made to calcine the powders under various heating/cooling rates (Fig. 1). In this connection, it is shown that the yield of PbZrO₃ phase did not vary significantly with different heating/cooling rates ranging from 10 to 30 °C/min, in good agreement with the early observation for the PbZrO₃ powders subjected to 0.5 h of vibro-milling time [19].

After establishing the optimum combination between vibromilling time and calcination condition, similar investigation was

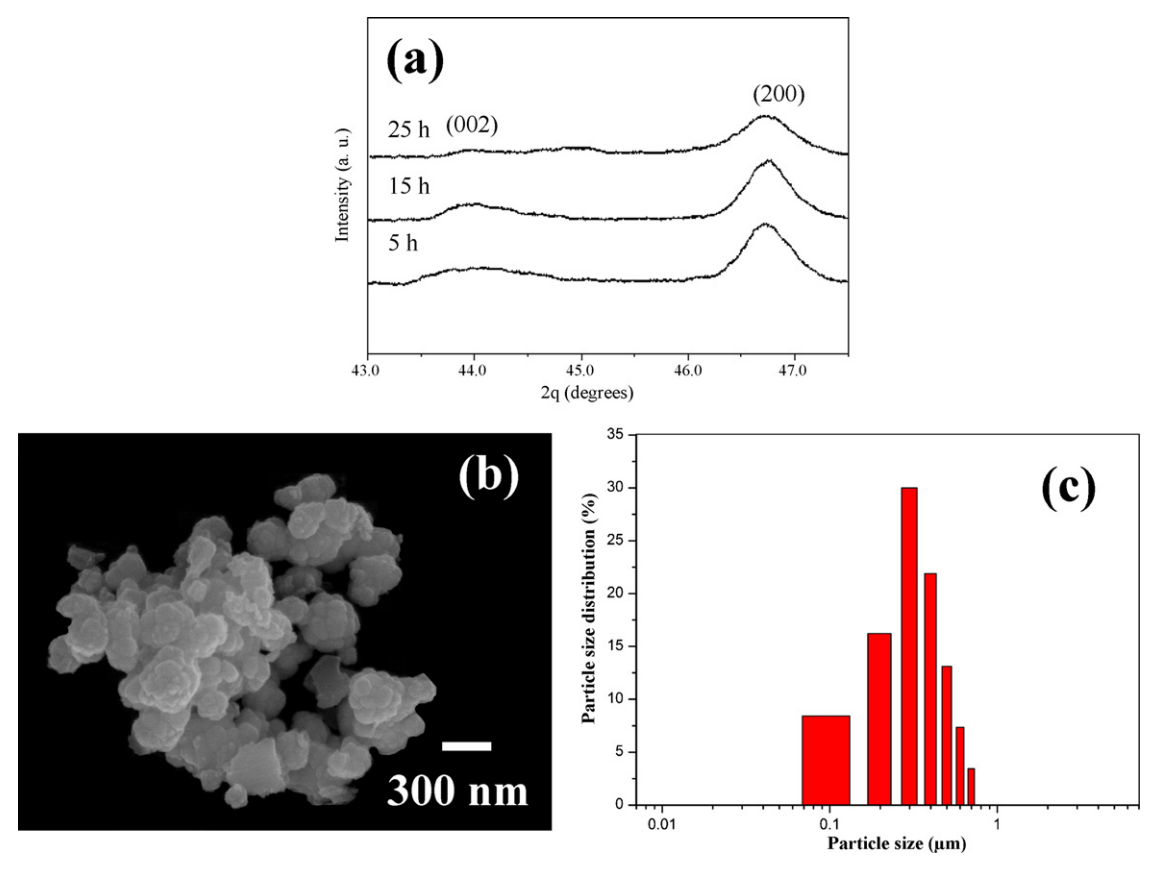


Fig. 3. (a) Enlarged zone of XRD patterns showing peaks broadening as a function of milling times of PT powders, (b) SEM micrograph and (c) particle size distribution of PT powders milled for $25 \, h$ and calcined at $600 \, ^{\circ} C$ for $1 \, h$ with heating/cooling rates of $30 \, ^{\circ} C$ /min.

also performed on the preparation of PbTiO₃ and BaTiO₃ powders as shown in Figs. 3 and 4, respectively. It should be noted that no evidences of the introduction of impurity due to wear debris from the selected milling process was observed in all calcined powders, indicating the effectiveness of the vibro-milling technique for the production of high purity nanopowders. Our previous investigations on related systems also indicated that no evidence of contamination from milling media was detected by XRD, EDX–SEM and TEM techniques [12,14,19,21,22]. As expected, there is evidence that, even for a wide range of calcination conditions, single-phase of all selected electroceramic powders cannot easily be produced, in agreement with literature [11–14]. This could be attributed mainly to the poor reactivity of starting species [13,14] and also the limited mixing capability of the mechanical method [23].

The variation of calculated crystallite size of all single-phase perovskite powders milled for different times and calcined at their optimum conditions is given in Table 1. In general, it is seen that the crystalline size of all powders decreases with increasing milling times. These observations indicate that the particle size affects the evolution of crystallinity of the phase formed by prolong milling treatment. Moreover, it has been observed that with increasing milling time, all diffraction lines broaden, as shown in Figs. 2(a), 3(a) and 4(a), which are an indication of a continuous decrease in particle size and of the introduction of lattice strain [15].

For all powders, the longer the milling time, the finer is the particle size. Also the relative intensities of the Bragg peaks and the calculated crystallite size for all powders tend to decrease with the increase of milling time. However, it is well documented that, as Scherer's analysis provides only a measurement of the extension of the coherently diffracting domains, the particle sizes estimated by this method can be significantly under estimated [14,15]. In addition to strain, factors, such as dislocations, stacking faults, heterogeneities in composition and instrumental broadening can contribute to peak broadening, making it almost impossible to extract a reliable particle size solely from XRD [15,23]. However, it should be noted that by increasing the calcination time from 1 to 4h, these calculated values decrease to the minimum at 2 h and then grow up further after more dwell time applied. There is no obvious interpretation of these observations, although it is likely to correspond to the competition between the major mechanisms leading to crystallization and agglomeration [19].

In this connection, a combination of SEM and laser diffraction techniques was also employed for the morphology and particle size distribution measurement, as some examples shown in Figs. 2(b,c), 3(b,c) and 4(b,c). In general, all powders are agglomerated and basically irregular in shape, with a substantial variation in particle sizes, particularly in powders subjected to high firing temperatures (Fig. 4(b)). The powders consist of primary particles of nanometers in size. The primary particles have

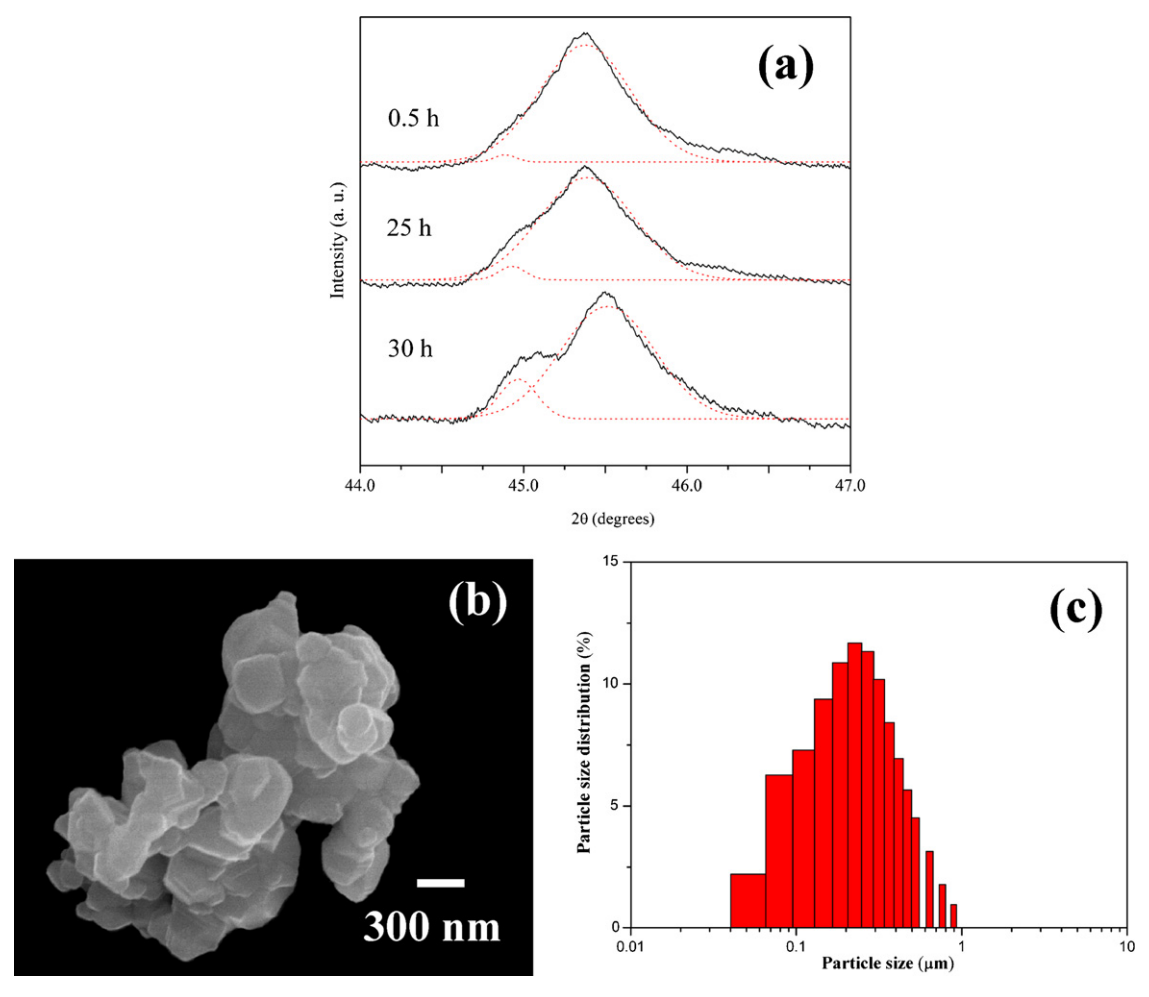


Fig. 4. (a) Enlarged zone of XRD patterns showing peaks broadening as a function of milling times of BT powders, (b) SEM micrograph and (c) particle size distribution of BT powders milled for $25 \, h$ and calcined at $1200 \, ^{\circ} C$ for $2 \, h$ with heating/cooling rates of $30 \, ^{\circ} C$ /min.

sizes of \sim 31–400, 17–109 and 250–700 nm, and the agglomerates measured \sim 35–750, 70–310 and 60–700 nm, for PZ, PT and BT powders, respectively. It is also of interest to point out that degree of agglomeration tends to increase with milling time and calcination temperatures (Fig. 4(b and c)), in good agreement with other works [12–14]. This observation may be attributed to the occurrence of hard agglomeration with strong inter-particle bond within each aggregates resulting from firing process. Any milling parameter, such as milling time, milling media or milling frequency, that influences the grain size within the particles has a corresponding effect on the resulting particle size.

The experimental work carried out here, suggests that mass production of single-phase PZ, PT and BT nanopowders with the smallest particle size $\sim 31,17$ and 100 nm, respectively (estimated from SEM micrographs), can be achieved by employing a combination of suitable vibro-milling time and calcination condition. Moreover, the employed heating/cooling rates for all selected powders observed in this work are also faster than those reported earlier [23–25]. In general, EDX analysis using a 20 nm probe on a large number of particles of these calcined electroceramic powders confirmed the existence of single (perovskite)-phase, in good agreement with XRD results.

4. Conclusions

Using commercially available oxide powders as the starting materials, this work demonstrated that a rapid vibro-milling technique has considerable potential for the low cost, large scale production of several high purity perovskite nanopowders. Through the suitable selection of milling time and calcination condition, the vibro-milling technique may be extended to the preparation of a very wide range of nanopowders.

Acknowledgements

This work was supported by the Thailand Research Fund (TRF), the Commission on Higher Education (CHE), National Nanotechnology Center (Nanotec), the Faculty of Science and the Graduate School of Chiang Mai University.

- [1] A.J. Moulson, J.M. Herbert, Electroceramics, second ed., Wiley, Chichester 2003
- [2] Y. Xu, Ferroelectric Materials and their Applications, North-Holland, New York, 1991.

- [3] G.H. Haertling, J. Am. Ceram. Soc. 82 (1999) 797–818.
- [4] D. Segal, Processing of ceramics, Part 1, in: R.J. Brook (Ed.), Materials Science and Technology, Verlagsgesellscaft mbH, Weinheim, 1996.
- [5] N. Setter, J. Eur. Ceram. Soc. 21 (2001) 1279-1293.
- [6] P.G. McCormick, T. Tsuzuki, J.S. Robinson, J. Ding, Adv. Mater. 13 (2001) 1008–1010.
- [7] D.D.E. Lakeman, D.A. Payne, Mater. Chem. Phys. 38 (1994) 305-324.
- [8] W.E. Rhine, K. Saegusa, R.B. Hallock, M.J. Cima, Ceram. Trans. 12 (1990) 107–118
- [9] A. Dias, V.T.L. Buono, V.S.T. Ciminelli, R.L. Moreira, J. Eur. Ceram. Soc. 19 (1999) 1027–1031.
- [10] M. Dambekalne, I. Brante, A. Sternberg, Ferroelectrics 90 (1989) 1–14.
- [11] S. Ananta, N.W. Thomas, J. Eur. Ceram. Soc. 19 (1999) 155–163.
- [12] R. Wongmaneerung, T. Sarakonsri, R. Yimnirun, S. Ananta, Mater. Sci. Eng. B 130 (2006) 246–253.
- [13] R. Wongmaneerung, R. Yimnirun, S. Ananta, Mater. Lett. 60 (2006) 1447–1452.
- [14] R. Wongmaneerung, R. Yimnirun, S. Ananta, Mater. Lett. 60 (2006) 2666–2671.

- [15] H. Klug, L. Alexander, X-ray Diffraction Procedures for Polycrystalline and Amorphous Materials, second ed., Wiley, New York, 1974.
- [16] JCPDS-ICDD Card no. 35-0739, International Centre for Diffraction Data, Newtown Square, PA, 2000.
- [17] S.D. Pradhan, S.D. Sathaye, K.R. Patil, A. Mitra, Mater. Lett. 48 (2001) 351–355
- [18] E.E. Oren, E. Taspinar, A.C. Tas, J. Am. Ceram. Soc. 80 (1997) 2714– 2716.
- [19] W. Chaisan, O. Khamman, R. Yimnirun, S. Ananta, J. Mater. Sci., in press.
- [20] JCPDS-ICDD Card no. 77-1971, International Centre for Diffraction Data, Newtown Square, PA, 2000.
- [21] R. Wongmaneerung, T. Sarnkonsri, R. Yimnirun, S. Ananta, Mater. Sci. Eng. B132 (2006) 292–299.
- [22] A. Prasatkhetragarn, R. Yimnirun, S. Ananta, Mater. Lett., in press.
- [23] A. Revesz, T. Ungar, A. Borbely, J. Lendvai, Nanostruct. Mater. 7 (1996) 779–788.
- [24] A. Udomporn, S. Ananta, Mater. Lett. 58 (2004) 1154-1159.
- [25] W. Chaisan, S. Ananta, T. Tunkasiri, Curr. Appl. Phys. 4 (2004) 182–185.

Effect of Annealing on the Structure and Dielectric Properties in PZT-PCoN Ceramics

N. Vittayakorn^{1,5,a}, N. Chaiyo¹, R. Muanghlua², A. Ruangphanit³ and W. C. Vittayakorn⁴

^a e-mail: naratipcmu@yahoo.com

Keyword: Ferroelectric Materials, Lead Zirconate Titanate, Lead Cobolt Niobate

Abstract The solid solution between the normal ferroelectric $Pb(Zr_{1/2}Ti_{1/2})O_3$ (PZT) and relaxor ferroelectric $Pb(Co_{1/3}Nb_{2/3})O_3$ (PCoN) was synthesized by the solid state reaction method. Sintered PZT-PCoN ceramics were annealed at temperatures ranging from 850 to 1,100°C for 4 h. X-ray diffraction patterns revealed changes of crystalline structure after annealing, which could be correlated to the accompanied changes in dielectric properties. Furthermore, significant improvements in the dielectric responses were observed in this system. After annealing, a huge increase of up to 200% occurred in the dielectric constants, especially near the temperature of maximum dielectric constant.

Introduction

Piezoelectric lead zirconate titanate (PZT) ceramic material has been widely used for transducer applications, due to its excellent piezoelectric properties, and was a candidate in a number of recent investigations [1, 2]. It is well known that PZT material is almost always used with a dopent, modifier or other chemical constituents to improve and optimize its basic properties for a particular application [1, 3]. Lead zirconate titanate ceramics and their solid solution, along with several complex perovskite oxides represented by Pb(B'B")O₃, have been investigated [4-6]. Among the various complex ferroelectric oxide materials, several niobates with transition temperatures below room temperature are $Pb(Mg_{1/3}Nb_{2/3})O_3$, $Pb(Ni_{1/3}Nb_{2/3})O_3$, and $Pb(Co_{1/3}Nb_{2/3})O_3$. Among them, lead cobalt niobate [Pb(Co_{1/3}Nb_{2/3})O₃ (PCoN)] is also a typical ferroelectric relaxor material with a transition temperature of -70°C, as reported by Smolenskii et al. [7] in 1958. In this compound, the octahedral sites of the crystal are occupied randomly by Co²⁺ and Nb⁵⁺ ions. Recently, our previous work has shown promise in producing phase pure perovskite PZT-PCoN ceramics with the solid state reaction method [5, 8]. A morphotropic phase boundary (MPB) between the PCoN-rich pseudo-cubic phase and the PZT-rich tetragonal phase reported $0.7Pb(Zr_{1/2}Ti_{1/2})O_3:0.3Pb(Co_{1/3}Nb_{2/3})O_3[5].$

In this study, we emphasized the effect of annealing on the crystal structure, and dielectric properties in PZT–PCoN ceramics. Based on our previous results for the PZT–PCoN system, PZT containing 30 mol% of PCoN was selected as the starting composition, which is close to the rhombohedral MPB in this system. For annealing, the samples were heat treated at 850-1,100°C for



¹ King Mongkut's Institute of Technology Ladkrabang Nanotechnology Research Center(NRC), King Mongkut's Institute of Technology Ladkrabang, Bangkok, Thailand 10520

²Electronics Research Center, Faculty of Engineering, King Mongkut's Institute of Technology Ladkrabang, Bangkok Thailand 10520

³ Department of Physics, Faculty of Science, Chiang Mai University, Chiang Mai, Thailand 50200

⁴ Thai Microelectronics Center (TMEC), National Electronics and Computer Technology Center, Nation Science and Technology Development Agency, Ministry of Science and Technology, Chachoengsao 24000, Thailand

Materials Science Research Unit, Department of Chemistry, Faculty of Science, King Mongkut's Institute of Technology Ladkrabang, Bangkok, Thailand 10520

4 hours in a sealed Al₂O₃ crucible, with PbO-rich atmosphere. This paper reports evolution of the perovskite phase, and crystal structure of the PZT–PCoN ceramics. Next, the temperature and frequency dependence of the dielectric constant are given for as-sintered and annealed samples. The results of influence on the post-sintering annealing of these properties are shown in brief.

Experiment

The 0.7Pb(Zr_{1/2}Ti_{1/2})O₃-0.3Pb(Co_{1/3}Nb_{2/3})O₃ ceramics were prepared by conventionally mixed-oxide processing, in which stoichiometric mixtures of reagent-grade metal oxide powders of 99% + purity (PbO, CoO, TiO₂, ZrO₂ and Nb₂O₅) were used as the starting raw materials. Thermal synthesis of blended and pressed mixture of the starting material was carried out at 900°C for a period of 4 h. Crumbled, milled and sieved material was pressed again in the form of cylinders and then sintered at 1,100°C for 4 h. The sintered pellets were then annealed at various temperatures from 850 to 1,100°C for 4 h. These annealing processes were performed in a double crucible, with interior PbO + ZrO₂ atmosphere, in order to maintain the established composition and, especially, avoid the loss of PbO caused by its sublimation. The Archimedes displacement method with distilled water was employed to evaluate sample density. The ceramic pellets were ground and polished to make parallel surfaces, and densities were determined geometrically. After gold sputtering onto the major faces of the pellets as electrodes, dielectric constants and losses at the frequency decades of 10 kHz were measured, using a computer-interfaced LCR meter.

Results and Discussions

The phase development in the annealed samples was analyzed by XRD and the results are presented in Figure 1. All samples show a single-phase powder diffraction pattern. No secondary reaction phases such as PbO, Pb-based compounds, unreacted oxide and so on, are observed in the pattern.

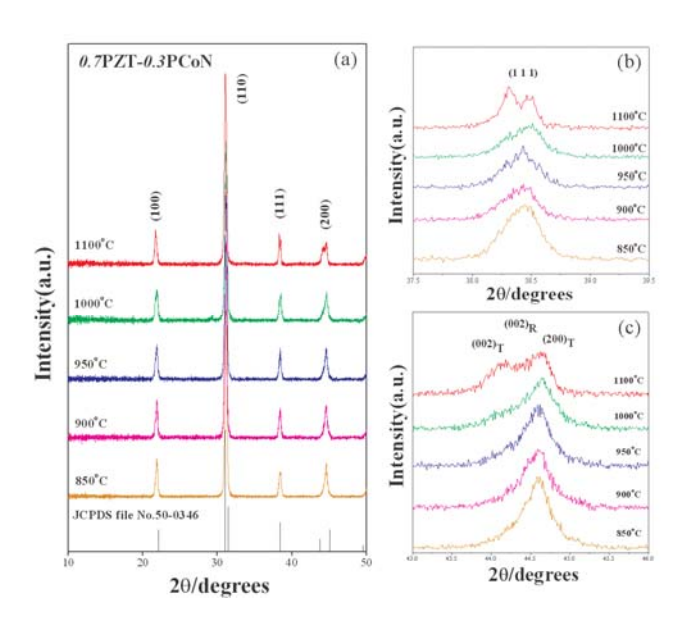


Figure 1 (a) XRD patterns of 0.7PZT-0.3PZN annealed samples at various temperatures for 4 h, (b) XRD pattern of the (1 1 1) peak, (c) XRD pattern of the (2 0 0) peak.

After annealing, a significant change in the crystal structure was observed, especially above an annealing temperature of $1,000^{\circ}$ C, where the crystal structure changes from pseudo-cubic to tetragonal and rhombohedral. On the basis of XRD and dielectric experiments, we have identified the MPB in the (1-x)PZT-xPCoN system from our previous work. The MPB resides at around $x \sim 0.2$, separating the tetragonal phase for $x \leq 0.2$ from the rhombohedral phase for $x \geq 0.3$. In this study, the XRD data show that splitting of the (200) and (111) peak is not observed in ceramic



samples annealed at temperatures below 1,000°C. These results indicated that the major phase in this ceramic sample had pseudo-cubic symmetry. Splitting of the (200) peak becomes more pronounced as the annealing temperature approaches 1,100°C, thus indicating stabilization of the tetragonal phase. Furthermore, the unambiguous splitting of the (111) peak indicated the coexistence of the rhombohedral and tetragonal phase. The co-existence of the tetragonal and rhombohedral phase is seen clearly when the XRD profile peak splits with increasing annealing temperature. From these results, it is clear that the composition of the annealed sample has shifted very closely to the MPB.

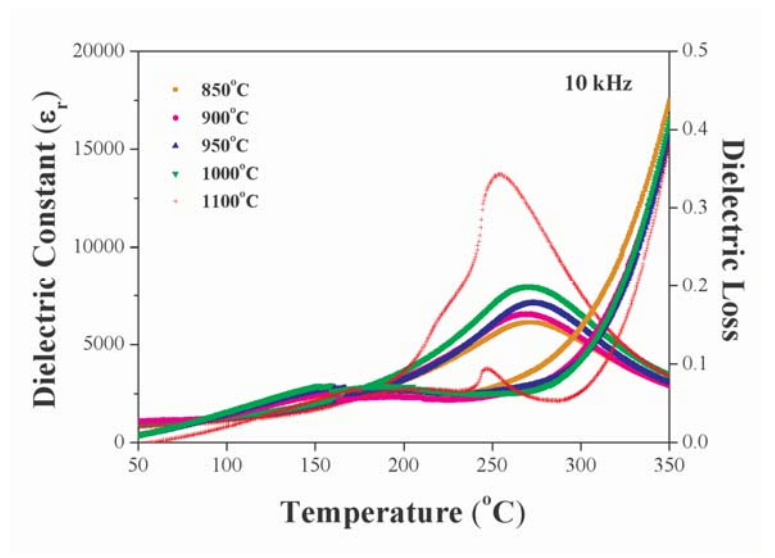
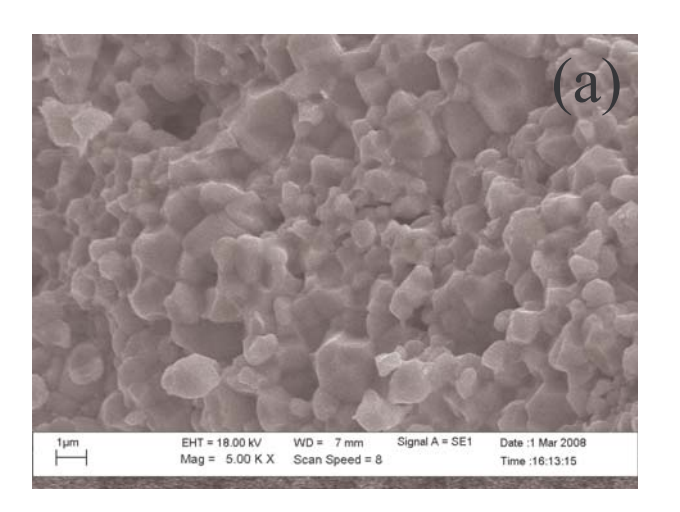


Figure 2 Variation of the dielectric constant (ε_r) and loss tangent $(\tan \delta)$ with different annealing temperatures at 10 kHz.



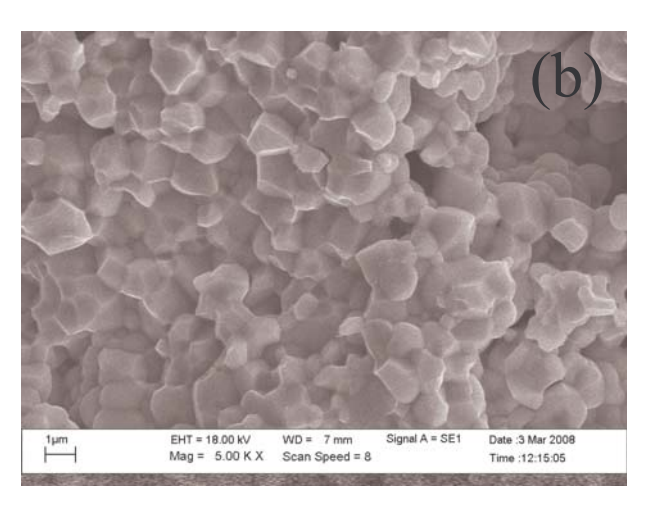


Figure 3 SEM photographs of 0.7PZT-0.3PCoN ceramics (a) as-sintered samples (b) annealing at 1,100°C.

Figure 2 shows the dielectric constant (ε_r) at 10 kHz versus the temperature for 0.7PZT-0.3PCoN ceramics annealed at different temperatures for 4 h. After annealing, a significant improvement in the dielectric constant was observed, especially near the temperature of the maximum dielectric constant (ε_m), where the improvement was up to 200%. This change in behavior might be due to a shift in a chemical composition close to the MPB, caused by thermal annealing. This behavior is consistent with the conclusions of Randall *et al.* [9]and Leite *et al.* [10] in the PMN–PT system. Figure 3 shows scanning electron microscopy (SEM) images of the fractured surfaces of 0.7PZT-



0.3PCoN ceramics before and after annealing at 1,100°C. There was no change in the grain size. The density of the samples decreased from 8.120 to 8.015 g/cm³ after annealing at 1,100°C for 4 h. Obviously, the decrease in density did not lead to an improvement of electrical responses.

Summary

The dielectric properties of 0.7PZT–0.3PCoN ceramics, formed via the solid state reaction, were investigated. Thermal annealing was seen to be effective at improving the dielectric and piezoelectric responses of PZT-based ferroelectric ceramics. The annealing time was found to have an effect on the electrical properties. After annealing at 1,100°C for 4h in a PbO-rich atmosphere, 0.7PZT-0.3PCoN ceramics with $\varepsilon_{\rm m}$ 14,400 were achieved in this study. The large improvements in dielectric properties after annealing were attributed to a shift in the phase composition to the MPB composition.

Acknowledgements

This work was supported by the Thailand Research Fund (TRF), the Commission on Higher Education (CHE), Thailand Graduate Institute of Science and Technology (TGIST), National Research Council of Thailand (NRCT) and King Mongkut's Institute of Technology Ladkrabang (KMITL).

- [1] G. H. Haertling: J. Am. Ceram. Soc. Vol. 82 (1999), p. 797.
- [2] K. Uchino: Ferroelectric Devices (Marcel Dekker, Inc., New York, 2000)
- [3] K. Uchino: Solid State Ionics Vol. 108 (1998), p. 43.
- [4] N. Vittayakorn, G. Rujijanagul, X. Tan, M. A. Marquardt and D. P. Cann: J. Appl. Phys. Vol. 96 (2004), p. 5103.
- [5] N. Vittayakorn and T. Tunkasiri: Phys. Scr. Vol. T129 (2007), p. 199.
- [6] N. Vittayakorn, G. Rujijanagul, X. Tan, H. He, M. A. Marquardt and D. P. Cann, J. Electroceramic Vol. 16 (2006), p. 141.
- [7] G. A. Smolenskii and A. L. Agranovskaya: Sov. Phys.-Tech. Phys. (1958), p. 1380.
- [8] N. Vittayakorn, S. Wirunchit, S. Traisak, R. Yimnirun and G. Rujijanagul: Curr. Appl Phys. Vol. 8 (2008), p. 128.
- [9] C. A. Randall, A. D. Hilton, D. J. Barber and T. R. Shrout: J. Mater. Res. Vol. 8 (1993), p. 880
- [10] E. R. Leite, A. M. Scotch, A. Khan, T. Li, H. M. Chan, M. P. Harmer, S.-F. Liu and S.-E. Park: J. Am. Ceram. Soc. Vol. 85 (2002), p. 3018.



Microstuctural Study and Properties of 0.8PZT-0.2BT Ceramics using a Two-stage Sintering Procedure

W. C. Vittayakorn

Department of Physics, Faculty of Science, Chiang Mai University, Chiang Mai, Thailand wanwilai_chaisan@yahoo.com

Keywords: Microstructure, Sintering, PZT, BT

Abstract. Lead zirconate titanate-barium titanate (0.8PZT-0.2BT) ceramic was prepared by conventional mixed-oxide method combined with a two-stage sintering procedure. A sintering time of 2 h at 1000 °C followed by a second step in the temperature range of 1000-1200 °C for 2 h was employed to the samples and compared to the one-step sintering process. Phase formation, densification and microstructure of all ceramics were examined via X-ray diffraction (XRD), Archimedes method and scanning electron microscope (SEM). The results lead to the conclusion that the pure perovskite phase and high densification of 0.8PZT-0.2BT ceramics with small grain can be successfully achieved under suitable two-stage sintering conditions.

Introduction

Nowadays, lead-based ferroelectric ceramics are widely applied in multilayer capacitors, transducers and sensors because of their excellent electrical properties [1]. Many of these applications require materials with superior electrical properties. Both PZT and BT are among the most common ferroelectric ceramics and have been studied extensively since the late 1940s [2, 3]. These two ceramics have distinct characteristics that make each ceramic suitable for different applications. The PZT ceramic has great piezoelectric properties which can be applied in transducer applications. Furthermore, it has a high $T_{\rm C}$ of 390 °C which allows electronic devices to be operated at high temperatures. BT ceramic is a normal ferroelectric material which exhibits a high dielectric constant, a lower $T_{\rm C}$ (~120 °C) and better mechanical properties [1-3]. However, sintering temperature of BT is higher than PZT. Thus, mixing PZT with BT is expected to decrease the sintering temperature of BT-based ceramics, a desirable move towards electrode of lower cost [4]. Moreover, since PZT-BT is not a pure-lead system, it is easier to prepare single phase ceramics with significantly lower amount of undesirable pyrochlore phases, usually associated with lead-based system [5, 6]. With their complimentary characteristics, it is expected that excellent electrical properties with preparation ease can be obtained from ceramics in PZT-BT system.

The electrical properties of ferroelectric ceramics depend strongly on microstructure as well as chemical compositions [1, 7]. It was reported earlier that the high value of dielectric constant can be revealed if polycrystalline ferroelectric ceramics of fine grain size is achieved [8, 9]. Thus, a fine grain is essential to attain optimum dielectric properties. In the literatures, it is well known that the microstructure of most ferroelectric ceramics can be normally controlled by two approaches. Utilizing additives to prohibit the grain growth is one approach [10-12]. Another approach uses novel processing technique to modify the microstructure. Numerous studies on the sintering process of ferroelectric ceramics have been reported in previous works [9, 13, 14]. Recently, a two-stage sintering method has been proposed by Chen and Wang to achieve the densification of ceramic bodies without significant grain growth [15]. Moreover, Kim and Han [9] found that intermediate dense and fine grain size BT ceramic was achieved from the two-stage sintering technique and showed much greater dielectric constant than that of the normal sintering technique. However, there is no systematic study about two-stage sintering on lead-based ferroelectric ceramics. Therefore, in this work a two-stage sintering method, which is a low-cost technique and simple ceramic fabrication to obtain highly dense ceramics, has been adopted to produce the fine



grain PZT-BT ceramic. The influence of two-stage sintering on densification and microstructure of the ceramics is investigated with comparison to the normal sintering scheme.

Experimental

0.8Pb(Zr_{0.52}Ti_{0.48})O₃-0.2BaTiO₃ powders used in this study were prepared by a simple mixed oxide synthetic route. Commercially available powders of PbO, ZrO₂, BaCO₃ and TiO₂, (Fluka, >99% purity) were used as starting materials. PZT and BT powders were first form in order to avoid unwanted pyrochlore phases. The 0.8PZT-0.2BT powders were then formulated from the PZT and BT components by employing the mixed-oxide procedure. The mixing process was carried out by ball-milled a mixture of raw materials for 24 h with corundum media in ethanol. After wet-milling, the slurry was dried at 120 °C and calcined in a closed alumina crucible, with the optimum calcination condition (1200 °C for 2 h). Ceramic fabrication was achieved by adding 1 wt% polyvinyl alcohol (PVA) binder, prior to pressing as pellets (15 mm of diameter and 1.0 mm of thickness) in an uniaxial die press at 100 MPa. Each pellet was placed in an alumina crucible together with atmosphere powders of identical chemical composition. In the so-called two-stage sintering process, the first sintering temperature (T₁) was assigned for 1000 °C and variation of the second sintering temperature (T₂) between 1000 °C and 1200 °C was carried out (Fig. 1). For comparison, normal sintering process was also carried out at the firing temperature between 1150 and 1350 °C for 2 h. The two sintering schemes also included the binder burn out process at 500 °C for 1 h. Phase formation of all ceramics was examined via X-ray diffraction (XRD). Densities of the final sintered products were determined by using the Archimedes principle. Microstructural development was characterized using a JEOL JSM-840A scanning electron microscopy (SEM).

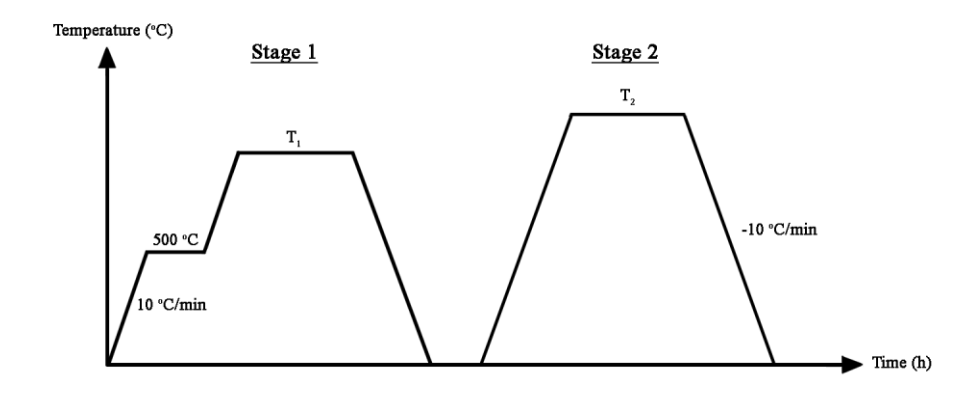


Fig. 1. A two-stage sintering procedure.

Results and Discussion

The XRD patterns of two-stage sintered 0.8PZT-0.2BT ceramic compared with normal sintered ceramic were illustrated in Fig. 2. The XRD graphs for both ceramics show almost the same. From Fig. 2, it can be indicated that the single phase of 0.8PZT-0.2BT (yield of 100% within the limitations of the XRD technique) was found in both samples. The ceramics were identified as perovskite structure having tetragonal symmetry and the diffraction peaks shifted towards to XRD pattern of tetragonal PZT which can be matched with the JCPDS file no. 33-0784. The cell parameter of each ceramic can be calculated using nonlinear least-square method. The cell parameters a = 0.4013 nm, c = 0.4071 nm can be achieved for normal sintered ceramics and a = 0.3994 nm, c = 0.4056 nm for two-stage sintered ceramic.

The microstructure of 0.8PZT-0.2BT ceramics with the highest density was revealed by SEM. Micrographs of samples sintered with different schemes are shown in Fig. 3. As shown in Fig. 3, SEM micrographs reveal that the both ceramics exhibit good densification and homogenous grain



size. For the normal sintered ceramic, the grain size varies greatly from 0.5 to 10 μ m. However, it can be noticed that the microstructure of the two-stage sintered ceramics (Fig. 3b) is slightly different from that of the normal sintered PZT-BT samples (Fig. 3a). The two-stage sintered ceramic contains smaller average grain size ($\sim 2.0~\mu$ m) and some degree of porosity is clearly seen. In the two-stage sintering process, the first sintering temperature was fixed at 1000 °C, for constant dwell time of 2 h and heating/cooling rates of 10 °C/min, while the second sintering temperature was varied from 1000 °C to 1200 °C. It is found that the relative density of the two-stage sintered ceramics increased significantly from 69 to 82 % with increasing sintering temperature, while grain size changed only slightly (about 1-5 μ m). However, in normal sintering process, while the highest relative density is about 99 %, but the highest grain size is about 10 μ m. From this observation, it can be said that the advantage of the two-stage sintering technique in producing small grain size of 0.8PZT-0.2BT ceramic is clearly signified. Although the average grain size of 0.8PZT-0.2BT ceramic prepared by two-stage sintering is small but the highest densification is not so effective (82%), this is the result of volatile PbO loss due to double firing at moderate temperature. However, the highest densification can be improved by designing the proper sintering temperature.

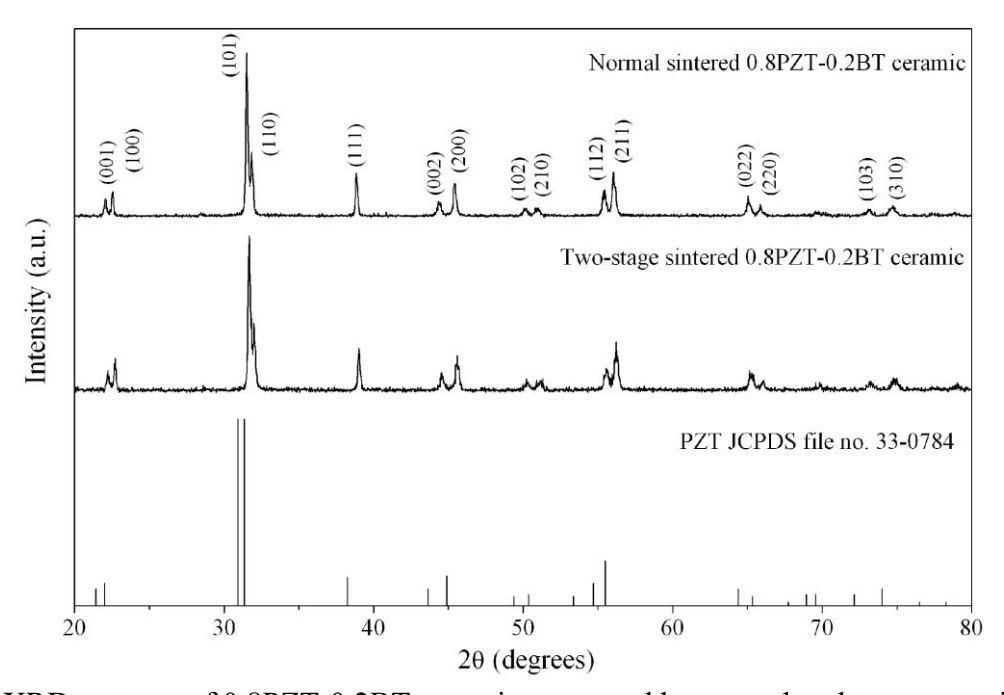


Fig. 2. XRD patterns of 0.8PZT-0.2BT ceramics prepared by normal and two-stage sintering.

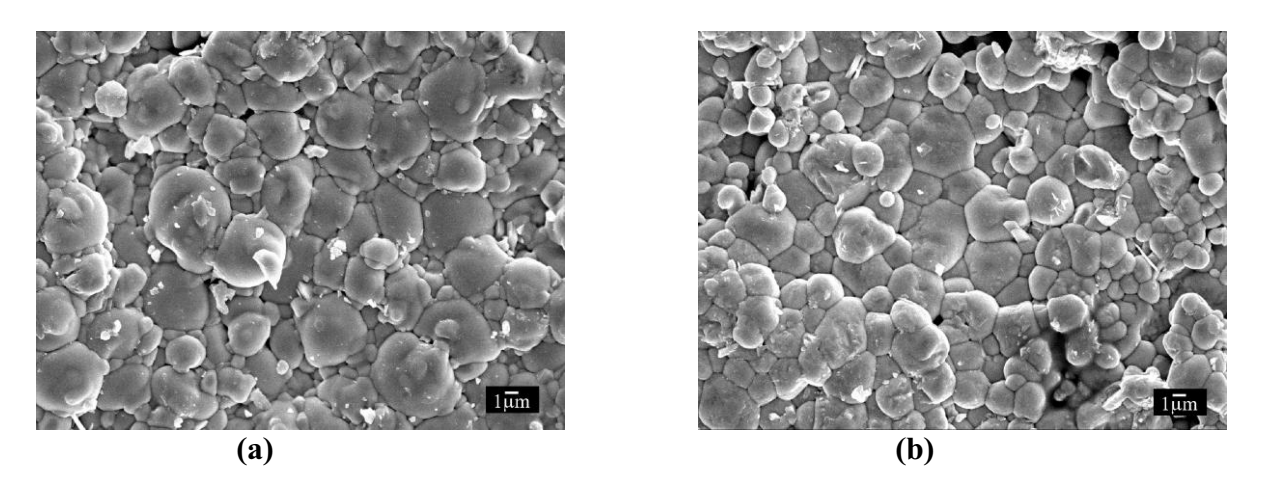


Fig. 3. SEM micrographs of 0.8PZT-0.2BT ceramics (a) normal sintered at 1300 °C and (b) two-stage sintered at 1000/1200 °C.



Even though exact mechanism of the microstructure observed here is not well established, but it should be noted that the various features of microstructure in PZT-BT ceramics are dependent on the grain growth rate in the different planes [16]. However, the sintering process and growth environment also play an important role in the formation [17]. More importantly, it can be assumed that the two-stage sintering process could suppress the grain growth mechanism efficiently whereas the relative density of both normal- and two-stage sintered ceramics is in high value. This can be explained that the feasibility of densification without grain growth, which is believed to occur in two-stage sintered ceramic, relies on the suppression of grain boundary migration while keeping grain boundary diffusion active. The kinetic and the driving force for grain growth behavior in the second-step sintering were previously discussed by Chen and Wang [15]. Their work suggested that the suppression of the final stage grain growth was achieved by exploiting the difference in kinetics between grain-boundary diffusion and grain-boundary migration.

Summary

Even though the simple mixed-oxide method employing a conventional ball-milling was used, this work demonstrated that it was possible to obtain smaller grain size ferroelectric PZT-BT ceramics with high densification by the two-stage sintering technique. It has been shown that, under suitable condition, two-stage sintering can effectively suppress the grain growth in 0.8PZT-0.2BT, leading to small-grained microstructure.

Acknowledgements

This work was supported by the Thailand Research Fund (TRF), Commission on Higher Education (CHE) and Faculty of Science of Chiang Mai University. I would also like to grateful to Assoc. Prof. Dr. Supon Ananta and Asst. Prof. Dr. Rattikorn Yimnirun from Department of Physics, Faculty of Science, CMU and Mr. Rangsan Muanghlua from Electronic Research Center, KMITL for all support.

- [1] A. J. Moulson and J. M. Herbert: *Electroceramics: Materials, Properties, Applications* (John Wiley & Sons Ltd., Chichester, 2003).
- [2] G. H. Haertling: J. Am. Ceram. Soc. Vol. 82 (1999), p. 797.
- [3] B. Jaffe, W. R. Cook and H. Jaffe: *Piezoelectric Ceramics* (Academic Press, London, 1971).
- [4] J. Chen, Z. Shen, F. Liu, X. Liu and J. Yun: Scripta Mater. Vol. 49 (2003), p. 509.
- [5] W. Chaisan, S. Ananta and T. Tunkasiri: Cur. Appl. Phys. Vol. 4 (2004), p. 182.
- [6] B. K. Gan, J. M. Xue, D. M. Wan and J. Wang: Appl. Phys. A Vol. 69 (1999), p. 433.
- [7] Y. Xu: Ferroelectric Materials and Their Applications (Elsevier Science Publishers B.V., 1991).
- [8] K. Kinoshita and A. Yamaji: J. Appl. Phys. Vol. 47 (1976), p. 371.
- [9] H. T. Kim and Y. H. Han: Ceram. Int. Vol. 30 (2004), p. 1719.
- [10] A. Yamaji, Y. Enomoto, K. Kinoshita and T. Murakami: J. Am. Ceram. Soc. Vol. 60 (1977), p. 97.
- [11] M. Kahn: J. Am. Ceram. Soc. Vol. 54 (1971), p. 452.
- [12] V. S. Tiwari, N. Singh and D. Pandey: J. Am. Ceram. Soc. Vol. 77 (1994), p. 1813.
- [13] J. S. Choi and H. G. Kim: J. Mater. Sci. Vol. 27 (1992), p. 1285.
- [14] J. K. Lee, K. S. Hong and J. W. Jang: J. Am. Ceram. Soc. Vol. 84 (2001), p. 2001.
- [15] I. W. Chen and X. H. Wang: Nature Vol. 404 (2000), p. 168.
- [16] M. H. Lin, J. F. Chou and H. Y. Lu: J. Eur. Ceram. Soc. Vol. 20 (2000), p. 517.
- [17] R. M. German: Sintering Theory and Practice (Wiley, New York, 1996).



Synthesis, Crystal Structures, Phase Transition Characterization and Thermal Properties of the (1-x)PbZrO₃-xPb(Co_{1/3}Nb_{2/3})O₃ Solid Solution System

W. Banlue¹, R. Muanghlua², W. C. Vittayakorn³ and N. Vittayakorn^{1,a}

¹Materials Science Research Unit, Faculty of Science, King Mongkut's Institute of Technology Ladkrabang, Bangkok, Thailand 10520

²Electronics Research Center, Faculty of Engineering, King Mongkut's Institute of Technology Ladkrabang, Bangkok Thailand 10520

Keyword: Antiferroelectric Materials, Ferroelectric, Lead Zirconate

Abstract The phase transition behavior of the (1-x) PbZrO₃-xPb(Co_{1/3}Nb_{2/3})O₃ (PZCN) solid solution system ($0 \le x \le 0.30$) has been investigated by X-ray diffraction and DSC. In the solid solution, for $x \le 0.20$, the transition shows a first-order phase transition behavior and its antiferroelectric (AFE) crystal structure is orthorhombic. The transition temperature gradually decreases with increased Co²⁺/Nb⁵⁺ concentration. On the composition range $0.20 \le x \le 0.30$, a typical relaxor-like behavior is displayed. The low temperature crystal structure is pseudo-cubic in this composition range. With these data, the ferroelectric phase diagram between PZ and PCoN has been established.

Introduction

Lead zirconate [PbZrO₃, abbreviated as PZ] is an antiferroelectric ceramic with a Curie temperature of 230°C [1, 2]. PZ is a parent compound of PbZr_{1-x}Ti_xO₃ (PZT) solid solutions, which are of high scientific and technological interest for their ferroelectricity and piezoelectricity observed over a wide range of compositions [3]. It is reported that the antiferroelectric (AFE) to ferroelectric transition (under the application of a strong electric field to the ceramic in the antiferroelectric state) leads to significant energy storage for the DC field [4]. This feature of PbZrO₃ makes it a candidate material for energy storage applications [3]. Lead cobolt niobate [Pb(Co_{1/3}Nb_{2/3})O₃, abbreviated as PCoN] is a relaxor ferroelectric, characterized by frequency-dependent dielectric maxima and a diffuse phase transition [5, 6]. The diffuse phase transition characteristic of the PCoN was first explained by Smolenskii and Agranovskaya on the basis of local compositional fluctuations on a microscopic scale [6, 7]. PCoN-based ceramics are considered to possess low sintering temperatures. Therefore, these materials can be applied for fabricating multilayer capacitors with low-temperature melting inner electrodes [8]. There have been many studies concerning the solid solution of PZ and other perovskite materials such as PbTiO₃ [9], BaZrO₃, [4, 10] PbSnO₃ [11] and SrZrO₃ [9]. However, to the best of the authors' knowledge, no work has been done on the solid solution between PZ and PCoN. Therefore, the objective of our present study is to investigate phase transition of (1-x)PbZrO₃ – xPb(Co_{1/3}Nb_{2/3})O₃ (PZ – PCoN) with x = 0.00 - 0.30 as a function of composition and temperature.

Experimental

The (1-x)PbZrO₃ – xPb(Co_{1/3}Nb_{2/3})O₃ ceramics, where x = 0.00, 0.02, 0.04, 0.06, 0.08, 0.10, 0.20 and 0.30, were prepared by a columbite precursor. First, a columbite (CoNb₂O₆) precursor was prepared using reagent-grade CoO and Nb₂O₅ in stoichiometric proportions. The powders were thoroughly mixed in a ball mill for 18 h, using ethanol as a grinding medium, and the mixed powder was calcined at 1,100°C for 4 h to obtain the columbite precursor. Single-phase formation of the



³ Department of Physics, Faculty of Science, Chiang Mai University, Chiang Mai, Thailand 50200 a naratipcmu@yahoo.com

precursor was confirmed by X-ray diffraction. The columbite precursor was mixed with PbO (99% purity), and ZrO₂ (99% purity) in different proportions for making different compositions, and each mix was calcined at 900°C for 4 h to acquire the desired composition of (1-x)PZ-xPCoN. Two mol percent of excess PbO was added to all the compositions to compensate for the lead loss during sintering. Single-phase formation was verified by powder XRD. Powders were compacted in disk form with a diameter of 15 mm and thickness of 2–3 mm. These disks were sintered in PbO-rich atmosphere at 1,150°C for 2 h. The densities of the sintered samples were measured to ~95% of the theoretical values. The crystal structure of the sintered pellets was determined by X-ray diffraction (XRD). The phase transition temperatures and enthalpy (Δ H) of the phase transitions were determined by DSC. This was operated from room temperature to 250°C with a heating rate of 10°C/min.

Results and Discussion

Figure 1 illustrates the XRD patterns of (1-x)PZ-xPCoN sintered pellets for $0.00 \le x \le 0.30$. It can be seen that the sintered pellets are single-phase: all the lines in each XRD pattern could be indexed with a perovskite cell. The diffraction peaks move gradually towards higher angles with increasing PCoN contents, indicating smaller cell parameters.

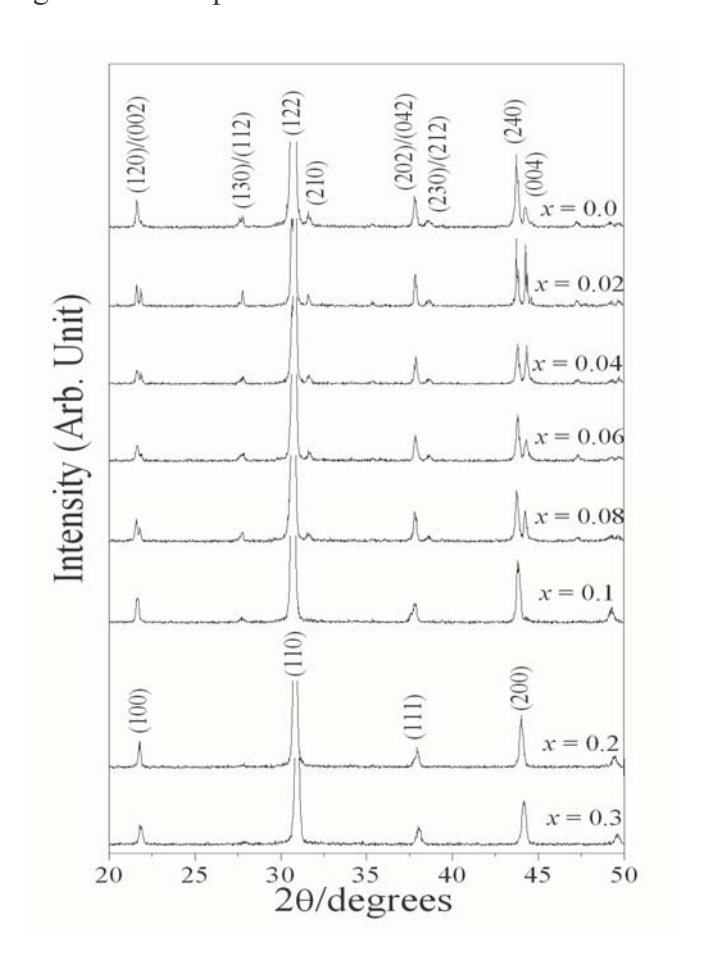


Figure 1 XRD patterns of (1-x)PbZrO₃ – xPb $(Co_{1/3}Nb_{2/3})O_3$ sintered pellets.



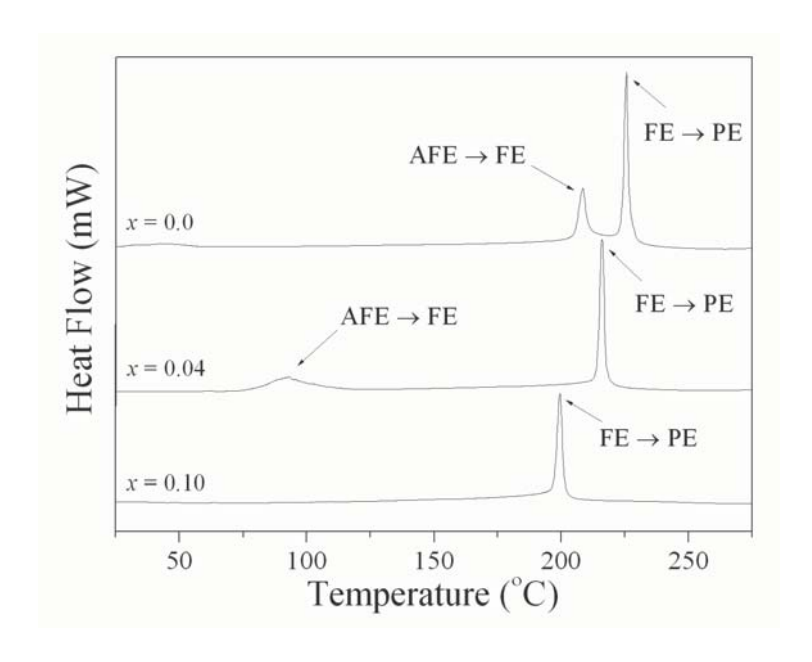


Figure 2 DSC thermographs of PZ-PCoN samples for: (a) x = 0, (b) x = 0.04 and (c) x = 0.10.

For the composition $0.00 \le x \le 0.10$, superstructure lines along with strong peaks are clearly observed, indicating that this composition belongs to the AFE orthorhombic phase. Furthermore, the samples with x = 0.1, 0.2 and 0.3 had a split (1 1 1) and (2 2 0) reflection and single (2 0 0) reflection, confirming that the crystal structure of the samples with x = 0.1, 0.2 and 0.3 is a rhombohedral perovskite. The DSC technique was used to investigate the phase transition of PZ-PCoN ceramics, with increasing PCoN concentration. A typical result of the DSC of PZ-PCoN for the composition x = 0, 0.04 and 0.10 is presented in Figure 2(a)-(c). Two distinct endothermic peaks observed for PZ at about 208.4 and 225.6°C are shown in Figure 2(a). The lower temperature corresponds to the transition temperature of the AFE phase transition, while the higher temperature corresponds to the FE

PE phase transition. In Figure 2(b), two endothermic peaks are shown at 92.8 and 216.1°C for the composition, x = 0.04. The AFE \rightarrow FE phase transition was found in the compositions of $0.00 \le x \le 0.10$. The peaks shift to lower temperatures, with a higher composition of x. This result corresponds to a decreasing AFE phase, with increasing amounts of PCoN content. Table 1 gives the transition temperature, including AFE→FE and FE→PE transitions of different PZ-PCoN compositions observed from DSC. The temperature range width of the FE phase increases progressively with PCoN content. After accumulating all these data, the ferroelectric phase diagram of (1-x)PZ-xPCoN has been finally established as a function of temperature and composition, as shown in Figure 3.

Table 1 Phase transitions temperature of (1-x)PZ-xPCoN ceramics

Composition	Phase transition temperature (°C)			
X	AFE→FE	FE→PE		
0.00	208.4	225.6		
0.02	145.2	220.9		
0.04	92.8	216.1		
0.06	33.3	209.9		
0.08	-	204.6		
0.10	-	199.4		
0.20	-	182.0		
0.30	-	158.2		



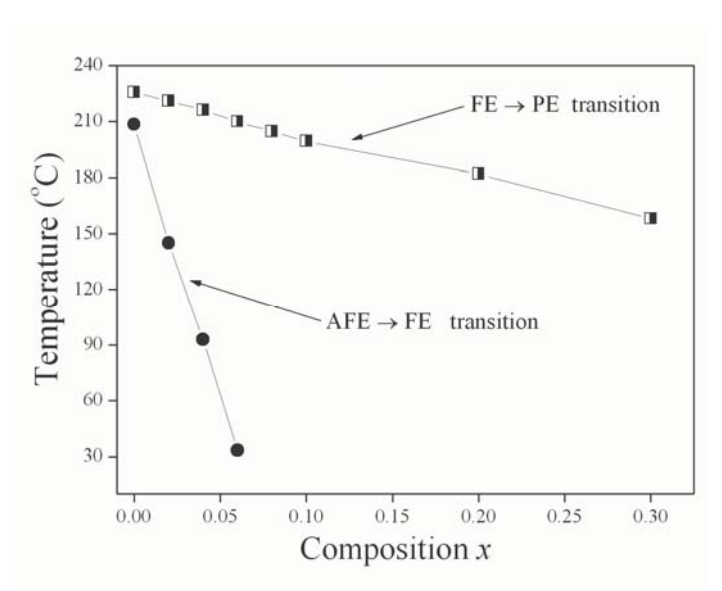


Figure 3 Ferroelectric phase diagram of the (1-x)PZ - xPCoN, x = 0.0-0.30 binary system.

The transition temperature decreases linearly with x, from approximately $T_c = 235^{\circ}C$ for x = 0.0 to $158.2^{\circ}C$ for x = 0.3. At room temperature, the phase boundary between the orthorhombic, antiferroelectric and rhombohedral ferroelectric phases was observed near x = 0.08. The phase diagram consists of three distinct crystallographic phases in this system; high temperature paraelectric cubic, rhombohedral, and ferroelectric orthorhombic.

Summary

Relaxor ferroelectric PCoN has been found to strongly influence crystal structure and thermal properties of PZ ceramics. The crystal structure data obtained from XRD indicate that the solid solution (I-x)PZ - xPCoN, where x = 0.0-0.3, successively transforms from orthorhombic to rhombohedral symmetry with increased PCoN concentration. The AFE \rightarrow FE phase transition is found in compositions of $0.0 \le x \le 0.08$. The AFE \rightarrow FE phase transition shifts to lower temperatures with higher compositions of x. The temperature range width of the FE phase increases with increased PCoN.

Acknowledgment

This work was supported by the Thailand Research Fund (TRF), the Commission on Higher Education (CHE), and King Mongkut's Institute of Technology Ladkrabang (KMITL).

- [1] E. Sawaguchi, G. Shirane and S. Hoshino: Phys. Rev. Vol. 83 (1951), p. 1078.
- [2] F. Jona, G. Shirane, F. Mazzi and R. Pepinsky: Phys. Rev. Vol. 105 (1957), p. 849.
- [3] G. H. Haertling: J. Am. Ceram. Soc. Vol. 82 (1999), p. 797.
- [4] B. P. Pokharel and D. Pandey: J. Appl. Phys. Vol. 86 (1999), p. 3327.
- [5] K. Uchino: Ferroelectrics Vol. 151 (1994), p. 321.
- [6] G. A. Smolenskii and Isupov: Sov. Phys. doklady. Vol. 9 (1954), p. 653.
- [7] N. Setter and L. E. Cross: J. Appl. Phys. Vol. 51 (1980), p. 4356.
- [8] A. Halliyal, U. Kumar, R. E. Newham and L. E. Cross: Am. Ceram. Soc. Bull. Vol. 66 (1987), p. 671.
- [9] B. Jaffe and W. R. Cook: *Piezoelectric ceramic* (R.A.N. Publishers, 1971).
- [10] B. P. Pokharel and D. Pandey, Phys. Rev. B. Vol. 65 (2002), p. 214108.
- [11] Y. Xu, Ferroelectric Materials and Their Application (Elsevier Science Publishers B.V., 1991).



Effects of Zr/Ti Ratio on the Structure and Ferroelectric Properties in PZT-PZN-PMN Ceramics Near the Morphotropic Phase Boundary

R. Muanghlua¹, S. Niemchareon ¹, W. C. Vittayakorn² and N. Vittayakorn^{3,a}

¹Electronics Research Center, Faculty of Engineering, King Mongkut's Institute of Technology Ladkrabang, Bangkok Thailand 10520

^a e-mail: naratipcmu@yahoo.com

Keyword: Ferroelectric Materials, Lead Zirconate titanate, Morphotropic phase boundary

Abstract The piezoelectric ceramics of $Pb(Zr_xTi_{1-x})O_3 - Pb(Zn_{1/3}Nb_{2/3})O_3 - Pb(Mn_{1/3}Nb_{2/3})O_3$; PZT-PZN-PMN with Zr/Ti ratios of 48/52, 50/50 and 52/48 were fabricated in order to investigate the effect of compositional modifications on the ferroelectric properties of PZT-PZN-PMN ceramics. The phase structure of ceramics sintered at 1,150°C was analyzed. Results show that the pure perovskite phase was in all ceramic specimens, and the phase structure of PZT-PZN-PMN piezoelectric ceramics transformed from tetragonal to rhombohedral, with the Zr/Ti ratios increased in the system. The PZT-PZN-PMN ceramics with a Zr/Ti ratio of 50/50 exhibited the most promising properties including high remanent polarization and low coercive field of 25.95 μ C cm⁻² and 12.5 kV cm⁻¹, respectively. Furthermore, the transition temperature decreased when the Zr/Ti ratio increased in the system.

Introduction

Lead zirconate titanate (PZT) is one of the most commonly used ferroelectric ceramic materials. The material has been studied intensively since discovery of the miscibility of lead titanate and lead zirconate in the 1950s. Due to their excellent dielectric, pyroelectric, piezoelectric and electro optic properties, they have a variety of applications in high energy capacitors, non-volatile memories (FRAM), ultrasonic sensors, infra red detectors, electro optic devices, and step-down multilayer piezoelectric transformers for AC–DC converter applications. Until now, many ternary and quaternary systems, such as PNW–PMN–PZT [1], PMN–PZN–PZT [2], PZT–PNN–PZN [3], and PZT–PFW–PMN [4] have been synthesized by modifications or substitutions to satisfy the requirements of the multilayered piezoelectric transformers. In this work, we studied influences of the Zr/Ti ratio on the crystal structure, and piezoelectric and dielectric properties of Pb(Zr_xTi_{1-x})O₃ – Pb(Zr_xTi_{1-x})O₃ –

Experimental

The powders and ceramics with compositions of $Pb_{0.97}Sr_{0.03}[(Mn_{1/3}Nb_{2/3})_{0.07}(Zn_{1/3}Nb_{2/3})_{0.06}(Zr_{(1-x)}Ti_x)_{0.87}]O_3$ were prepared via a conventional mixed-oxide process, where x=0.48, 0.50 and 0.52. Reagent-grade oxide powders PbO (99.0%), ZrO_2 (99.0%), TiO_2 (99.5%), Nb_2O_5 (99.5%), ZnO(99.9%) and MnO_2 (99.0%) were mixed, consecutively. The mixtures were milled in ethanol using zirconium ball as media in a polyethylene jar for 18 h. The mixed slurry was dried at 80°C and calcined at 850°C for 4 h. Then, the calcined powders were ground again under the same condition in order to obtain fine uniform powders. After drying, the powders were added to 5 wt.% polyvinyl alcohol (PVA) solution, and then pressed into 15 mm diameter plates under a pressure of 100 MPa. The pressed plates were sintered at 950–1,100°C for 6 h in a sealed alumina crucible with lead atmosphere. The sintered ceramics were examined by X-ray diffractometry (XRD, D8



Department of Physics, Faculty of Science, Chiang Mai University, Chiang Mai, Thailand 50200
 Materials Science Research Unit, Faculty of Science, King Mongkut's Institute of Technology Ladkrabang, Bangkok, Thailand 10520

Advance) to determine the phase structure. Subsequently, the sintered disks were polished, and silver-paste electrodes were fired at 850° C. In addition, the polarization (P) was measured as a function of electric field (E), using a ferroelectric tester system (Radiant Technologies, Inc., PT66A).

Results and Discussion

Figure 1 (a) and (b) show the XRD patterns of $Pb_{0.97}Sr_{0.03}[(Mn_{1/3}Nb_{2/3})_{0.07}(Zn_{1/3}Nb_{2/3})_{0.06}(Zr_{(1-x)}Ti_x)_{0.87}]O_3$ sintered pellets for x=0.48, 0.50 and 0.52. The sintered pellets can be seen as a single-phase: all the lines in each XRD pattern could be indexed with a perovskite cell. No secondary reaction phases, such as PbO, Pb-based compounds, unreacted oxide and so on, are observed in the pattern.

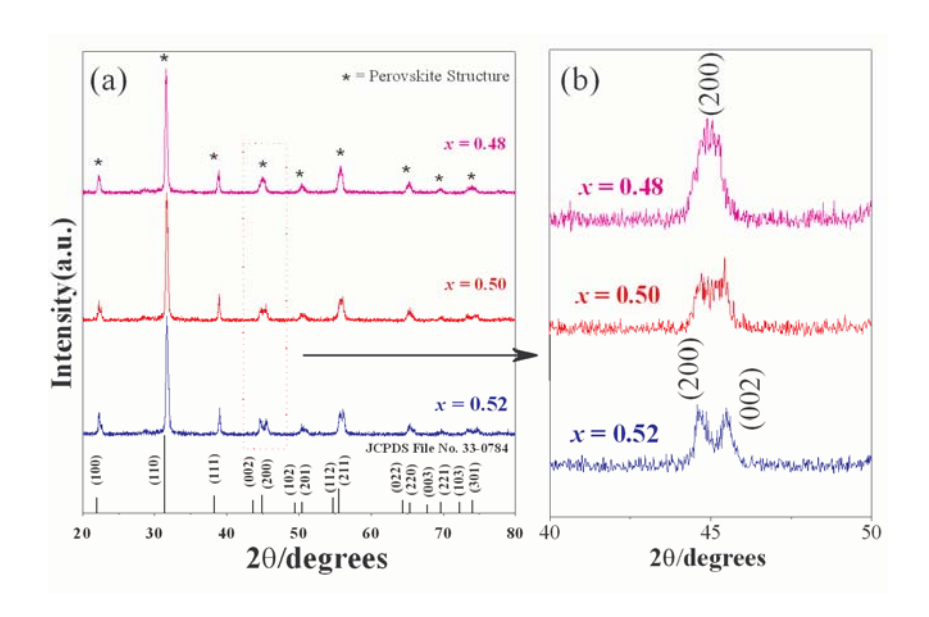


Figure 1 XRD patterns of $Pb_{0.97}Sr_{0.03}[(Mn_{1/3}Nb_{2/3})_{0.07}(Zn_{1/3}Nb_{2/3})_{0.06}(Zr_{(1-x)}Ti_x)_{0.87}]O_3$ sintered pellets.

Based on the careful XRD study of $(2\ 0\ 0)$ reflections in Figure 1(b), we found that a phase transformation from the pseudo-cubic structure to the tetragonal structure occurs with increasing x content. The ceramics with x=0.48 exist as a pseudo-cubic phase revealed by the single $(2\ 0\ 0)_R$ peak. At x=0.50, the ceramics coexist as a tetragonal and pseudo-cubic phase revealed by the coexistence of $(0\ 0\ 2)_T$ and $(2\ 0\ 0)_R$ peaks in the 2θ range of 43.5° to 45.5° . The ceramics exist as a tetragonal phase when indicated by the splitting of $(0\ 0\ 2)$ and $(2\ 0\ 0)$ peaks in the 2θ range of 43.5° to 46.5° at x=0.52.

Table 1 Characteristics of $Pb_{0.97}Sr_{0.03}[(Mn_{1/3}Nb_{2/3})_{0.07}(Zn_{1/3}Nb_{2/3})_{0.06}(Zr_{(1-x)}Ti_x)_{0.87}]O_3$ ceramics with optimized processing conditions

Composition <i>x</i>	Crystal structure	Theoretical Density (%)	Grain Size (µm)
0.48	PC	94.05	2.84
0.50	PC+T	94.03	2.72
0.52	PC	95.21	2.94



In the first approximation, it could be said that the composition between x=0.50 is close to the morphotropic phase boundary (MPB) of this system, where the structure of the $Pb_{0.97}Sr_{0.03}[(Mn_{1/3}Nb_{2/3})_{0.07}(Zn_{1/3}Nb_{2/3})_{0.06}(Zr_{(1-x)}Ti_x)_{0.87}]O_3$ compositions is gradually changing from pseudo-cubic to tetragonal. The physical properties do not vary significantly with the ceramic compositions, as listed in Table 1.

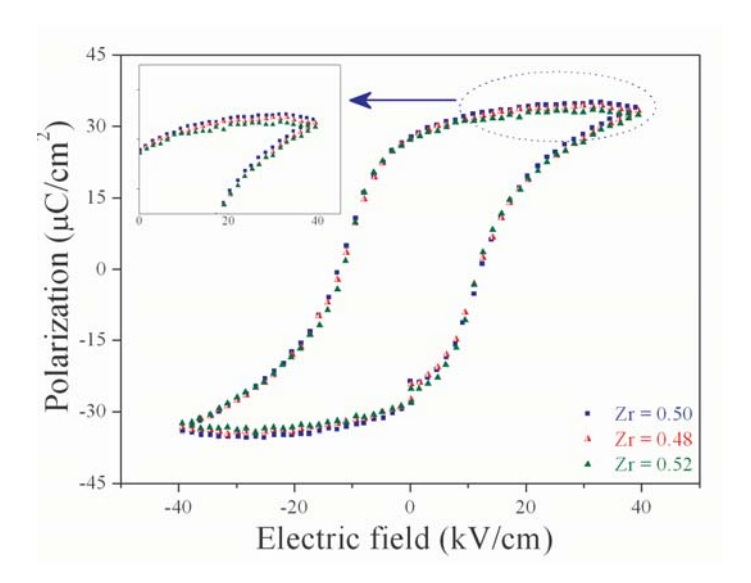


Figure 2 Hysteresis loops of the $Pb_{0.97}Sr_{0.03}[(Mn_{1/3}Nb_{2/3})_{0.07}(Zn_{1/3}Nb_{2/3})_{0.06}(Zr_{(1-x)}Ti_x)_{0.87}]O_3$ ceramics with x = 0.48, 0.50 and 0.52 measured at 40 kV/cm.

Figure 2 illustrates the P–E curves of the samples, with x = 0.48, 0.50 and 0.52 measured at 25 kV/cm. All compositions show symmetry in shape and reveal rectangular hysteresis loops, which is typical of a phase that contains long-range cooperation between dipoles. No evidence of pinning effect or asymmetric loop was detected in any electric field strengths. From the fully saturated loops, the remanent polarization P_r and coercive field E_c were determined. The values of P_r and E_c for composition x = 0.50 are 25.95 μ C/cm² and 12.5 kV/cm, respectively, whereas the remanent polarization P_r is 25.7 μ C/cm² for composition x = 0.48. Maximum remanent polarization was observed in the ceramic with composition x = 0.5. It has been seen that the samples with compositions x = 0.5 exhibit the highest saturation and remnant polarization among all the ceramics studied. As indicated by the above XRD, the composition with x = 0.5 contains both tetragonal and pseudo-cubic phases, so it should favor a strong ferroelectric effect. This is due to the increased ease of reorientation during poling by the transformation of a number of 180° domains into 90° ones. Also revealed from these results, the MPB coexisting in the tetragonal and pseudo-cubic phases in the present system is a broad composition region of x = 0.5, which exhibits high ferroelectric properties around the center of the MPB.

Summary

The Zr/Ti ratio has been found to influence crystal structure and ferroelectric properties of $Pb_{0.97}Sr_{0.03}[(Mn_{1/3}Nb_{2/3})_{0.07}(Zn_{1/3}Nb_{2/3})_{0.06}(Zr_{(1-x)}Ti_x)_{0.87}]O_3$ ceramics. The crystal structure data obtained from XRD indicate that the solid solution $Pb_{0.97}Sr_{0.03}[(Mn_{1/3}Nb_{2/3})_{0.07}(Zn_{1/3}Nb_{2/3})_{0.06}(Zr_{(1-x)}Ti_x)_{0.87}]$, where x=0.48, 0.50 and 0.52, successively transforms from pseudo-cubic to tetragonal symmetry with increased x concentration. More interestingly, XRD analysis and ferroelectric property measurements indicated the existence of the MPB composition at between x=0.50.



Acknowledgment

This work was supported by the Thailand Research Fund (TRF), the Commission on Higher Education (CHE), and Faculty of Engineering, King Mongkut's Institute of Technology Ladkrabang and King Mongkut's Institute of Technology Ladkrabang (KMITL).

- [1] Z. Yang, R. Zhang, L. Yang and Y. Chang: Materials Research Bulletin. Vol. 42 (2007), p. 2156.
- [2] J. Yoo, K. Kim, C. Lee, L. Hwang, D. Paik, H. Yoon and H. Choi: Sensors and Actuators A: Physical. Vol. 137 (2007), p. 81.
- [3] N. Vittayakorn and D. P. Cann; Appl. Phys. A. Vol. 86 (2007), p. 403.
- [4] Z. Yang, X. Chao, C. Kang and R. Zhang: Materials Research Bulletin. Vol. 43 (2008), p. 38.



Synthesis, Phase Formation and Characterization of Co₄Nb₂O₉ Powders Synthesized by Solid-State Reaction

N. Chaiyo¹, R. Muanghlua², A. Ruangphanit³, W. C. Vittayakorn⁴ and N. Vittayakorn^{1,5,a}

- ¹ King Mongkut's Institute of Technology Ladkrabang Nanotechnology Research Center (NRC), King Mongkut's Institute of Technology Ladkrabang, Bangkok, Thailand 10520
- ²Electronics Research Center, Faculty of Engineering, King Mongkut's Institute of Technology Ladkrabang, Bangkok Thailand 10520
- ³ Thai Microelectronics Center (TMEC), National Electronics and Computer Technology Center, Nation Science and Technology Development Agency, Ministry of Science and Technology, Chachoengsao 24000, Thailand
- ⁴ Department of Physics, Faculty of Science, Chiang Mai University, Chiang Mai, Thailand 50200
- Materials Science Research Unit, Department of Chemistry, Faculty of Science, King Mongkut's Institute of Technology Ladkrabang, Bangkok, Thailand 10520

^a e-mail: naratipcmu@yahoo.com

Keywords: Co₄Nb₂O₉; Calcinations; Powder synthesis; Microwave dielectric

Abstract. A corundum-type structure of cobalt niobate $(Co_4Nb_2O_9)$ has been synthesized by a solid-state reaction. The formation of the $Co_4Nb_2O_9$ phase in the calcined powders was investigated as a function of calcination conditions by differential thermal analysis (DTA) and X-ray diffraction (XRD) techniques. Morphology and particle size have been determined by scanning electron microscopy (SEM). It was found that the minor phases of unreacted Co_3O_4 tend to form together with the columbite $CoNb_2O_6$ phase at a low calcination temperature and short dwell time. It seems that the single-phase of $Co_4Nb_2O_9$ in a corundum phase can be obtained successfully at the calcination conditions of $900^{\circ}C$ for 60 min, with heating/cooling rates of $20^{\circ}C$ /min.

Introduction

A variety of microwave dielectric ceramics have been utilized for microwave dielectric applications including the filters and resonators in the wireless communication system [1]. There are three important properties required, i.e., a high dielectric constant ε_r , high quality factor $Q \times f$ and low temperature coefficient of resonant frequency τ_f , in order to miniaturize the size of the microwave dielectric resonator and reach suitability for application at high frequency, and the resonant frequency must be stable at various operating temperatures. A high $Q \times f$ value of more than 30,000 GHz is required to withstand high electric loads, especially for microwave dielectric ceramics used in the base stations of mobile phones. However, still higher $Q \times f$ – value materials are required for new digital systems [2]. Over the past few years, the demand for smaller, lighter and temperature stable devices has increased. Cobalt niobate CoNb₂O₆ is one of the best known microwave dielectric materials, which recently gained considerable attention. In general, production of single-phase CoNb₂O₆ is not straightforward, as a minor concentration of Co₄Nb₂O₉ sometimes forms alongside the major phase of CoNb₂O₆. The crystal structure of Co₄Nb₂O₉ ceramic is known to have a corundum-type structure. The oxygen ions are located at the lattice sites of a hexagonal closed-packed unit cell. In the HCP crystal structure, as in the FCC structure, there are as many octahedral interstitial sites as there are atoms in the unit cell. In recent study, the microwave dielectric properties of a corundum-type structure such as Mg₄Nb₂O₉ ceramic was reported to have a high $Q \times f$ value, which was comparable to that of Al₂O₃. Thus far, although Co₄Nb₂O₉ is identical



in stoichiometry to Mg₄Nb₂O₉, it has not been synthesized to the corundum-type structure. Interestingly, the mixed oxide route for the production of Co₄Nb₂O₉ powders has not received detailed attention, and the effects of calcination conditions have not yet been studied extensively. The objective of this work was to study the reaction between the starting cobalt oxide and niobium oxide precursors, phase formation and microstructure of corundum-type structure cobalt niobate powder.

Experimental

Reagent-grade oxides of Co_3O_4 (99.99 %, Aldrich, USA) and Nb_2O_5 (99.9%, Aldrich, USA) were used in this study. $Co_4Nb_2O_9$ powders were synthesized by the solid-state reaction of Co_3O_4 and Nb_2O_5 powders that were homogenized by ball milling with ethyl alcohol in the required stoichiometric ratio. The mixed slurry was dried at 80° C. The reactions of the uncalcined $Co_4Nb_2O_9$ powder, taking place during heat treatment, were investigated by differential thermal analysis (DTA; Perkin-Elmer 7 series) using a heating rate of 10° C /min in air from room temperature to 1,350 °C. According to the DTA results, various calcination conditions (i.e. temperatures ranging from 700 – 1,100 °C and dwell times from 15 to 240 min) were applied, with a heating/cooling rate of 20° C/min in order to investigate the formation of $Co_4Nb_2O_9$. Calcined powders were subsequently examined by room temperature X-ray diffraction (XRD; Bruker D8 Advance) using Ni-filtered CuK_{α} radiation to identify the phase formed and optimum calcination condition for the formation of $Co_4Nb_2O_9$ powders. Powder morphologies and grain size were directly imaged using scanning electron microscopy (LEO, LEO 1455VP, Cambridge, England).

Results and Discussion

The DTA curve for the powder mixed in the stoichiometric proportions of $Co_4Nb_2O_9$ is shown in Figure 1. Three endothermic peaks centered at $121^{\circ}C$, $294^{\circ}C$ and $837^{\circ}C$ were observed. The first and second endothermic peaks should correspond to the evaporation of water molecules and decomposition of the organic species from the milling process, respectively [3, 4]. The third endothermic peak, at $837^{\circ}C$, was assigned to the formation of $Co_4Nb_2O_9$ by combination reactions of Co_3O_4 and Nb_2O_5 . Based on the DTA measurements, these data were used to define the range of calcination temperature at between 700 to 1,100 $^{\circ}C$ for XRD investigation.

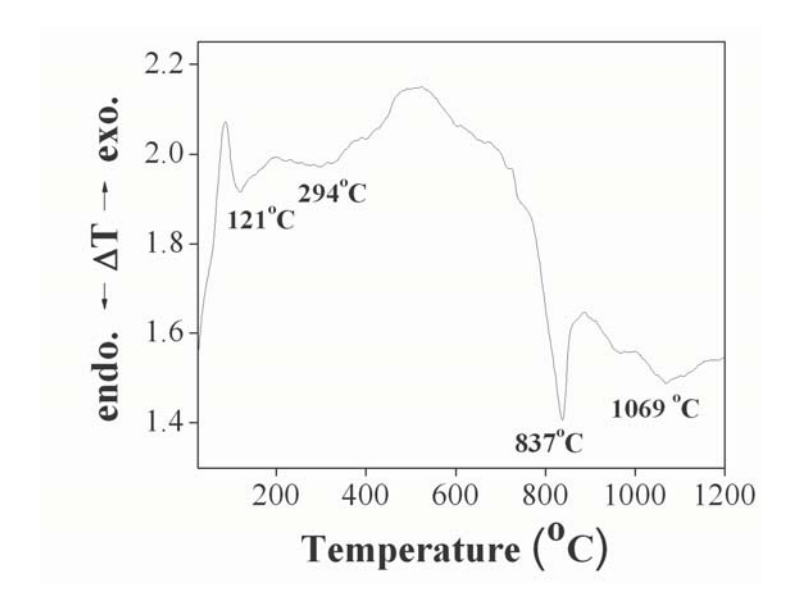


Figure 1. DTA curve for the mixture of Co₃O₄-Nb₂O₅ powder.



XRD patterns of all calcined powders are given in Figure 2. At a clacination temperature as low as 800°C, the strongest reflections were apparent in the majority of the XRD patterns, which indicated the formation of a columbite phase of $CoNb_2O_6$ (A) that could be matched with JCPDS file numbers 32-0304. The minor phase of unreacted cubic- Co_3O_4 (Y), which could be matched with JCPDS files No 78-1969, were found. As the calcination temperature increased to 900°C, intensity of the corundum $Co_4Nb_2O_9$ peaks was enhanced further and became the monophasic phase. This $Co_4Nb_2O_9$ phase was indexable according to a hexagonal corundum-type structure, with a lattice parameter of a = 517 pm and c = 1412 pm, and space group P3c1 (no. 165), consistent with JCPDS file numbers 38-1457. Upon calcinations at 1,000 and 1,100 °C, an essentially monophasic phase of $Co_4Nb_2O_9$ was obtained. However, in this work, there were no significant differences between the powders calcined at temperatures ranging from 900 to 1,100 °C.

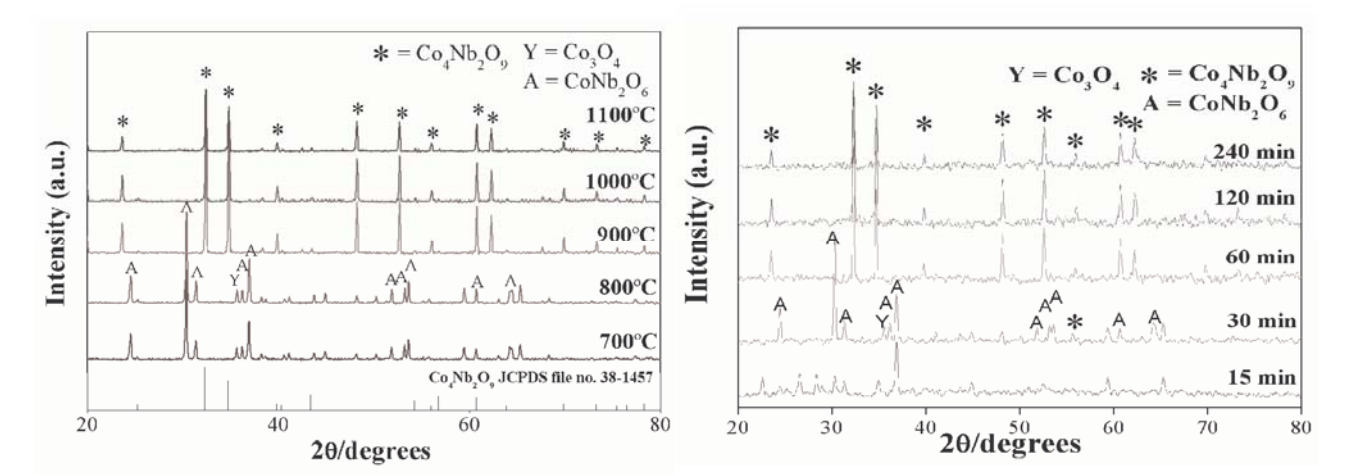


Figure 2. XRD patterns of Co₄Nb₂O₉ powder calcined at various temperatures for 4 h with heating/cooling rates of 20 °C /min.

Figure 3. XRD patterns of Co₄Nb₂O₉ powder calcined with heating/cooling rates of 20 °C /min at 900 °C for 15-240 min.

After obtaining the optimum calcination temperature, dwell times ranging from 15 min to 120 min, with a constant heating/cooling rate of 20°C/min were applied at 900 °C, as shown in Figure 3. It was observed that the single-phase of Co₄Nb₂O₉ (yield of 100% within the limitations of the XRD technique) powder was possible in powders calcined at 900°C, with a dwell time of 60 min or more applied. Observation that the dwell time effect may also play an important role in obtaining a single-phase product is also consistent with other systems [5, 6].

The average grain sizes were determined from the XRD pattern according to the Scherrer's equation

$$D = \frac{k\lambda}{\beta\cos\theta_B}$$

where D is the average grain size, k is a constant equal to 0.89, θ_B is the (3 1 1) peak angle, λ is the X-ray wavelength equal to 1.5406 Å and β is the half peak width. The average grain size of Co₄Nb₂O₉ powders was about 280 nm at 900 °C, with a dwell time of 60 min. The morphology of the calcined Co₄Nb₂O₉ powders was investigated by scanning electron microscopy (SEM), which is illustrated in Figure 4(a) and 4(b). In general, the particles are agglomerated and basically irregular in shape, with a substantial variation in particle size and morphology. The particle size can be estimated in the range of 300-400 nm from SEM micrographs. A detailed study at higher



magnification [Fig. 5(b)] shows that the particles had spherical secondary particles, composed of nano-sized primary particulates.

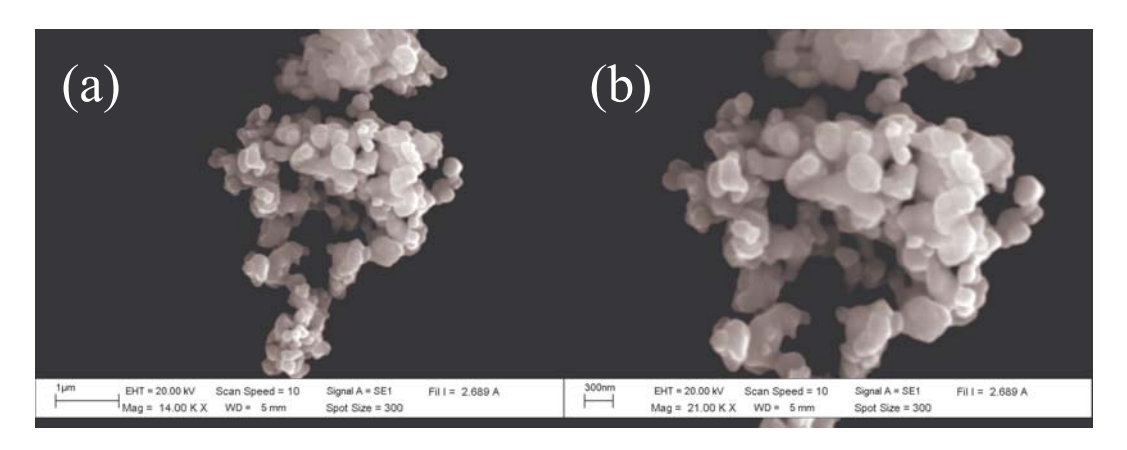


Figure 4. Scanning electron micrographs of the Co₄Nb₂O₉ powders calcined at 900 °C for 60 min, with a heating/cooling rate of 20 °C /min.

Summary

The corundum-structure, $Co_4Nb_2O_9$, was synthesized by solid state reaction using oxides as starting materials. The content of the impurity phases decreased with increasing calcination temperature and dwell time. Evidence has been obtained of a 100% yield of $Co_4Nb_2O_9$ at a calcination temperature of 900°C for 60 min, with heating/cooling rates of 20°C/minute. XRD showed the compound to have a corundum structure, with hexagonal lattice parameters of a = 5.1669(\pm 0.0014) and c = 14.1248 (\pm 0.0072). The particle size can be estimated in the range of 300-400 nm from SEM micrographs.

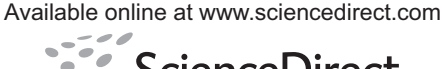
Acknowledgements

This work was supported by the Thailand Research Fund (TRF), the Commission on Higher Education (CHE), Thailand Graduate Institute of Science and Technology (TGIST), National Research Council of Thailand (NRCT) and King Mongkut's Institute of Technology Ladkrabang (KMITL).

- [1] A. Kan, H. Ogawa, A. Yokoi and Y. Nakamura: J. Euro. Ceram. Soc. Vol. 27 (2007), p. 2977.
- [2] A. J. Moulson and J. M. Herbert: *Electroceramics: Materials, Properties, Applications* (Chapman and Hall, New York, 1990)
- [3] S. Ananta, Mater. Lett. Vol. 58 (2004), p. 2530.
- [4] R. Wongmaneerung, T. Sarakonsri, R. Yimnirun and S. Ananta: Materials Science and Engineering: B. Vol. 130 (2006), p. 246.
- [5] R. Wongmaneerung, R. Yimnirun and S. Ananta: Mater. Lett. Vol. 60 (2006), p. 2666.
- [6] S. Wongsaenmai, R. Yimnirun and S. Ananta: Mater. Lett. Vol. 61 (2007), p. 2426.







ScienceDirect

Ceramics International 35 (2009) 121-124

INTERNATIONA

CERAMICS

www.elsevier.com/locate/ceramint

Preparation and characterization of ceramic nanocomposites in the PZT-BT system

Wanwilai Chaisan*, Rattikorn Yimnirun, Supon Ananta

Department of Physics, Faculty of Science, Chiang Mai University, Chiang Mai 50200, Thailand Accepted 1 October 2007 Available online 23 February 2008

Abstract

Nanocomposites of the (1 - x)PZT-xBT system were fabricated by the bimodal particle concept. The effect of fabricating conditions on structural characteristics and dielectric properties of the ceramics was investigated using XRD, SEM, and a standard dielectric measurement. The ceramic-solid solutions and -nanocomposites in the PZT-BT system were comparatively explored. It was clearly seen that the microstructures and the dielectric properties of PZT-BT ceramic-nanocomposites are totally different from those of ceramic-solid solutions. The dielectric behavior of ceramic-nanocomposites displayed superimposition of two phase transitions with a lower maximum value of the dielectric constant than that of the solid solutions.

© 2008 Elsevier Ltd and Techna Group S.r.l. All rights reserved.

Keywords: B. Nanocomposites; C. Dielectric properties; D. PZT; BT

1. Introduction

Piezoelectric ceramics (e.g. $Pb(Zr_x,Ti_{(1-x)})O_3$, $BaTiO_3$ and its related compounds), which are widely used as transducers, pressure sensors and actuators, suffer from mechanical and electrical deterioration in service because of fatigue damage. When piezoelectric devices are used in severe circumstances, such as high stress or high power applications, problems that are related to reliability (i.e. degradation of electrical properties and fatigue fracture) become more critical and important. Therefore, it is necessary to investigate the electrical behavior of piezoelectric ceramics and to design microstructure that possesses excellent electrical properties. Both BaTiO₃ (BT) and Pb(Zr,Ti)O₃ (PZT) are among the most common ferroelectric materials and have been studied extensively since the late 1940s [1,2]. These two ceramics have distinct characteristics that make each individual ceramic suitable for different applications. The compound PZT has highly desirable piezoelectric properties which can be applied in transducer applications. Furthermore, it has a high $T_{\rm C}$ of 390 °C which allows piezoelectric devices to be operated at relatively high temperatures. BT is a normal ferroelectric material which exhibits a high dielectric constant, a lower $T_{\rm C}$ (~120 °C) and better mechanical properties [1–3]. Thus, mixing PZT with BT is expected to decrease the sintering temperature of BT-based ceramics, allowing a desirable move towards electrodes of lower cost [4]. Moreover, the nano-reinforced structure is believed to improve densification and mechanical properties of the ceramic composite. Therefore, ceramic-nanocomposites of the lead zirconate titanate-barium titanate ((1 - x)PZT-xBT)system with various compositions, were fabricated using a modified mixed-oxide synthetic route and a bimodal particle concept. The effect of processing parameters on the arrangement of phases, microstructural evolution and electrical properties of the ceramics was carefully investigated using XRD, SEM and dielectric measurements.

2. Experimental procedure

Ceramic-nanocomposites in the system (1 - x)PZT-xBT $(0.1 \le x \le 0.5; \ \Delta x = 0.1)$ have been fabricated from PZT powder and BT nanopowder, employing a normal sintering method. Reagent grade PbO, ZrO₂, TiO₂ and BaCO₃ powders (Fluka, >99% purity) were used as starting materials. Powder of each end member (PZT and BT) was first formed in order to avoid unwanted pyrochlore phases. For the preparation of BT

^{*} Corresponding author. Tel.: +66 53 943367; fax: +66 53 943445. E-mail address: wanwilai_chaisan@yahoo.com (W. Chaisan).

nanopowder, a vibratory laboratory mill (McCrone Micronizing Mill) powered by a 1/30 HP motor was employed for 30 h with zirconia media in ethanol. The well-mixed powder was calcined at 1300 °C for 2 h in an alumina crucible. With a modified mixed-oxide method [5], the PZT powders were prepared using a lead zirconate (PbZrO₃) as precursor in order to reduce the occurrence of undesirable phase. Pure PbZrO₃ phase was first formed by reacting PbO with ZrO₂ at 800 °C for 2 h. PbZrO₃ powder was then mixed with PbO and TiO₂ and milled, dried and calcined at 900 °C for 2 h to form single phase PZT.

The (1-x)PZT-xBT mixed powders were then formulated from the BT and PZT components by employing the similar mixed-oxide procedure. In the mixing process, the calculated relevant proportions of constituents were weighed, suspended in ethanol and intimately mixed in a ball-mill with zirconia media. Drying was carried out for 2 h and the dried powder was then ground into the fine powders. The powders were then isostatically cold-pressed into pellets with a diameter of 15 mm and a thickness of 2 mm at a pressure of 4 MPa and sintered at 1200 °C for 2 h.

Densities of sintered ceramics were measured by Archimedes method and X-ray diffraction (XRD using CuK_{α} radiation) was employed to identify the phases formed. The grain morphology and size were directly imaged using scanning electron microscopy (SEM). For electrical measurements, silver paste was fired on both sides of the polished samples at 750 °C for 12 min as the electrodes. Dielectric properties of the sintered ceramics were studied as a function of both temperature and frequency. The capacitance was measured with a HP4284A LCR meter in connection with a Delta Design 9023 temperature chamber and a sample holder capable of high temperature measurement. Dielectric constant (ε_r) was calculated using the geometric area and thickness of the discs.

3. Results and discussion

XRD patterns of all sintered ceramic-nanocomposites are shown in Fig. 1. Here the peak positions and intensities of the XRD patterns vary according to the amount and chemical composition of the phases present. It is seen that the diffraction peaks shifted towards a higher angle with increasing x and the XRD peaks of all ceramic-nanocomposites are broader than those of solid-solution case in our earlier work [6]. These can be interpreted in terms of co-existing perovskite phases, i.e. PZT, BT and their reacted intermediate phases. Moreover, with careful observation, it is found that the sintered samples of $0.3 \le x \le 0.5$ nanocomposites exhibit the perovskite structure with traces of unwanted phase (∇) occurring at $2\theta \sim 28^{\circ}$. It is believed that this unwanted phase is ZrO₂ matched with JCPDS file no. 37-1484 [7]. Compositional fluctuations due to the evaporation of lead oxide within surface regions are believed to be responsible for the occurrence of free ZrO2 phase in the sintered (1 - x)PZT-xBT ceramics of $0.3 \le x \le 0.5$ nanocomposites. Another possibility was put forward by Fushimi and Ikeda [8], who suggested that melting of PT-PZ solid solution can change from congruent to incongruent and induce ZrO2 to

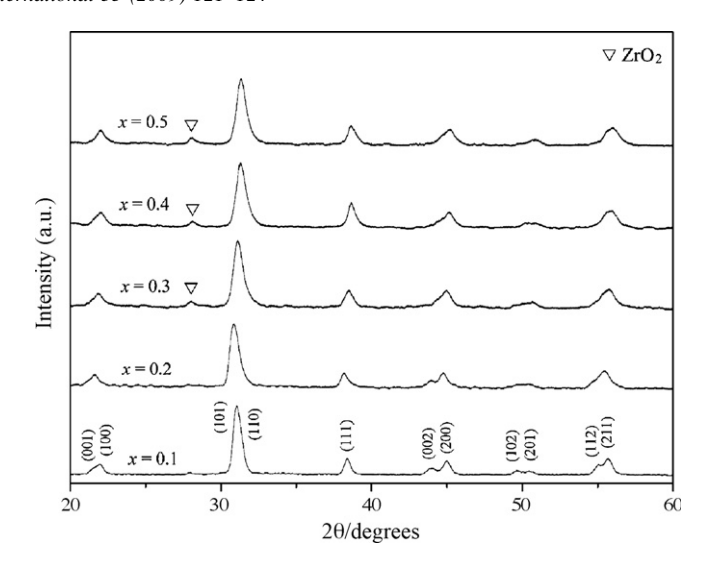


Fig. 1. XRD patterns of the (1 - x)PZT-xBT ceramic-nanocomposites sintered at 1200 °C for 2 h.

form at ~ 1340 °C. On the other hand, Brankovic et al. [9] suggested that incomplete reaction of the starting precursors can also result in the persistence of free ZrO_2 phase. Since no trace of ZrO_2 has been observed for sintered samples of x = 0.1 and 0.2, it is believed that the segregation of ZrO_2 may be associated with loss of Pb content and also depend on the level of BT content, similar with observations made in other perovskite systems [10,11].

The microstructural morphology of (1-x)PZT-xBT ceramic-nanocomposites was initially examined by SEM. Micrographs of as-fired surface of all ceramic-nanocomposites are shown in Fig. 2(a–e). In general, high porosity, heterogeneous microstructures consisting mainly of two ranges of particles (in respect of size and shape) were found in all samples. A distribution of very small spherical BT particles (brighter phase with diameter \sim 200–500 nm) is found over the PZT grains, especially for rich-BT samples. Large pore-sizes of the order of 2 μ m were also observed. These poorly sintered samples could be attributed to several factors, including the effect of different particle size fractions between the two end components, ineffective mixing and the use of low density green bodies produced by conventional uniaxial die-pressing.

Densities in the range 4.80–6.21 g/cm³ were obtained, which are considerably lower than the values obtained for sintered PZT–BT solid solution ceramics in our earlier work [6]. In order to preserve the ceramics with a nanostructural arrangement, it is possible that the sintering temperature employed in this work is not enough for driving the densification mechanism to achieve dense PZT/BT ceramicnanocomposites. However, so far, there are no reports on the production of highly dense PZT/BT ceramic-nanocomposites by a pressureless sintering method. Moreover, the scope for improving pressureless sintering by raising the temperature is limited by the melting point of PZT (~1400 °C) whilst the hotpressing technique can cause severe PbO-volatilization problems [12].

The temperature dependence of the dielectric constant (ε_r) measured at 1 MHz for (1 - x)PZT–xBT nanocomposites with

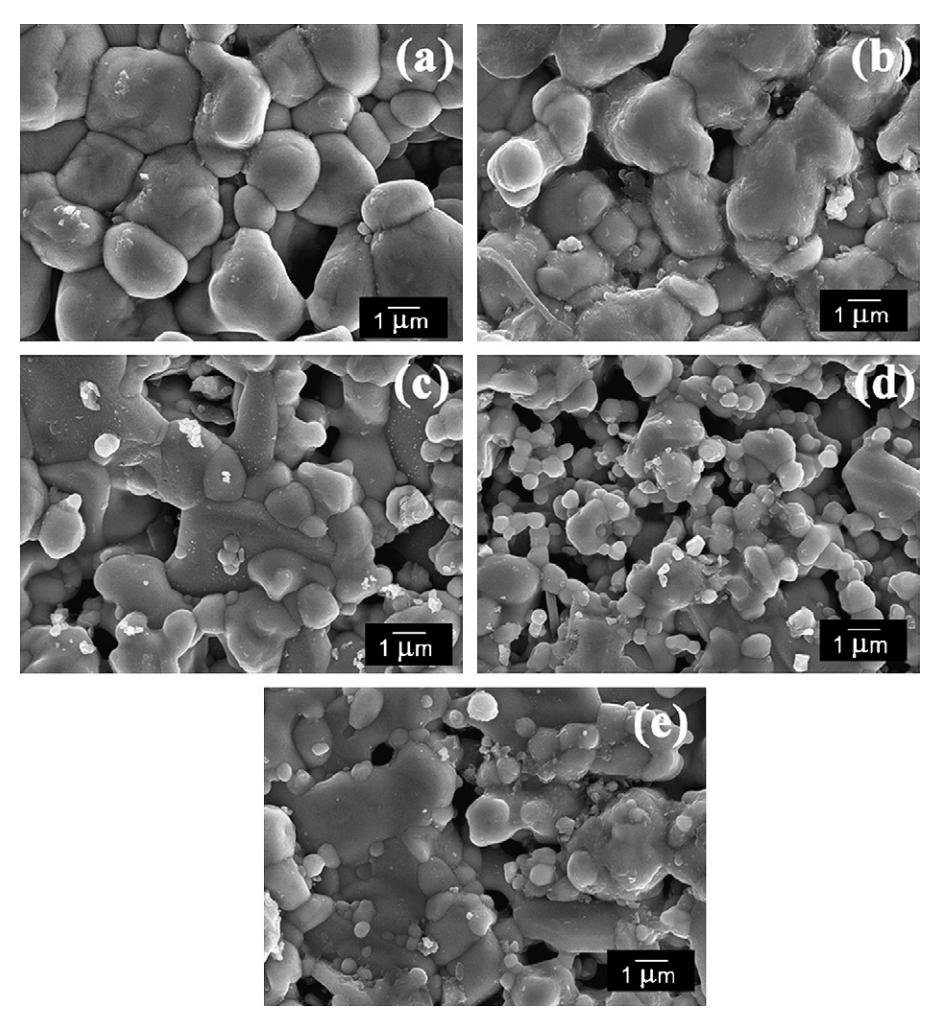


Fig. 2. SEM micrographs of as-fired surfaces of the sintered (1 - x)PZT-xBT ceramic-nanocomposites with $x = (a) \ 0.1$, $(b) \ 0.2$, $(c) \ 0.3$, $(d) \ 0.4$ and $(e) \ 0.5$.

 $0.1 \le x \le 0.5$ is shown in Fig. 3. All ceramic-nanocomposites display dielectric peak superimposition of the two phase transitions (T_1 and T_2) with no frequency dependence. The shape of dielectric peak for each composition seems to be the two peaks merged into a mound. The height of the mound was

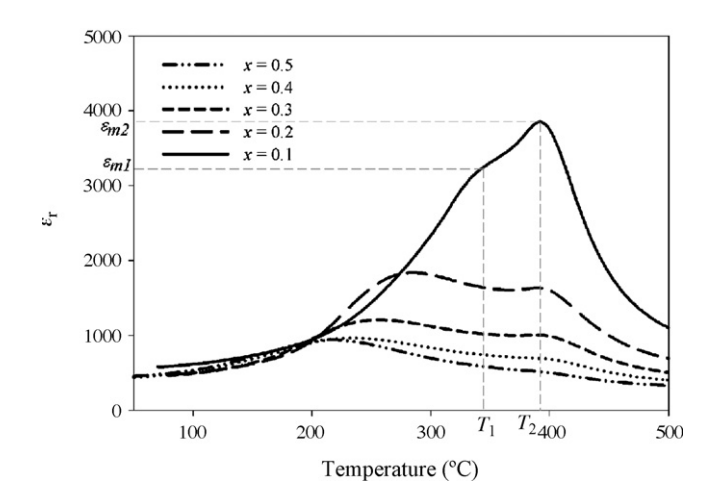


Fig. 3. Comparison of dielectric constant (e_r) at 1 MHz for (1-x)PZT-xBT ceramic-nanocomposites.

lower than those of solid solutions [6]. The phase transition temperatures, T_1 and T_2 , and dielectric data are illustrated in Fig. 3 and list in Table 1. As is well known, the dielectric constant of pure PZT and pure BT showed anomalies at 390 and 130 °C, respectively. Therefore, ceramic-nanocomposites between PZT and BT are expected to show a transition temperature between 390 and 130 °C. An attempt was made to characterize the dielectric temperature of PZT–BT as a function of x. However, difficulties were encountered in indexing the measured dielectric peak broadening obtained. As seen in Fig. 3, with increasing of x, T_1 and T_2 decrease moving toward

Table 1 Dielectric properties of ceramic-nanocomposites in the (1 - x)PZT-xBT system

Compositions (x)	<i>T</i> ₁ (°C)	$\varepsilon_{\mathrm{m1}}$	<i>T</i> ₂ (°C)	ε_{m2}
0.1	340	3200	392	3800
0.2	285	1800	390	1600
0.3	257	1200	388	1000
0.4	234	960	385	700
0.5	216	940	380	530

 $\varepsilon_{\rm m1}$ and $\varepsilon_{\rm m2}$ are the maximum dielectric constant at T_1 and T_2 , respectively (see also Fig. 3).

the Curie temperature of BT. T_1 refers to transition temperature of BT and T_2 refers to transition temperature of PZT. There are various proposals for explaining the dielectric response of composite materials. Ausloos [13] studied effective dielectric constant theories of composite solids. Their work reported that the broad spectrum of dielectric constant is the results of clustering effects, the shape of particle (or cluster) effect and particle heterogeneity effect. In this work, it is possible that the incorporation of BT nanoparticles into a PZT matrix may hinder domain wall motion sufficiently to reduce the dielectric constant [14]. Moreover, the presence of unwanted ZrO₂ phase (confirmed by XRD) and high porosity (confirmed by SEM) are other reasons for the low dielectric constants in ceramic-nanocomposites with composition of x > 0.2. However, by neglect accounting for the porosity, the maximum dielectric constant $(\varepsilon_{\rm max})$ of all ceramic-nanocomposites was back-calculated to 100% density for a better comparison with the solid solutions. Although the dielectric values of ceramic-nanocomposites are still lower than those of the solid solutions, the broadening is greater which infers the operating temperature with the moderate dielectric constant (\sim 1000–4000) of these ceramics is much wider in range, suitable for certain electronic devices.

4. Conclusions

Ceramics-nanocomposites in the system (1 - x)PZT-xBT were successfully processes by employing the bimodal particle concept. All PZT-BT compositions in this study were of the perovskite structure with tetragonal symmetry. The dielectric properties of all the ceramic-nanocomposites are strongly influenced by the presence of secondary phases and densification mechanism. The dielectric peak shows superimposition of the two phase transitions with no frequency dependence and the dielectric value is lower than that of solid solutions for all compositions, explained by theory of the dielectric response for composite materials. With increasing of x, the phase transition temperatures of all ceramics decrease moving toward to Curie temperature of BT.

Acknowledgement

I would like to thank the Thailand Research Fund (TRF), Commission on Higher Education (CHE) and the Faculty of Science, Chiang Mai University for all financial support.

- [1] G.H. Haertling, Ferroelectric ceramics: history and technology, J. Am. Ceram. Soc. 82 (4) (1999) 797–818.
- [2] B. Jaffe, W.R. Cook, H. Jaffe, Piezoelectric Ceramics, Academic Press, London, 1971.
- [3] A.J. Moulson, J.M. Herbert, Electroceramics: Materials, Properties, Applications, John Wiley & Sons Ltd., Chichester, 2003.
- [4] J. Chen, Z. Shen, F. Liu, X. Liu, J. Yun, Preparation and properties of barium titanate nanopowder by conventional and high-gravity reactive precipitation methods, Scripta Mater. 49 (2003) 509–514.
- [5] W. Chaisan, S. Ananta, T. Tunkasiri, Synthesis of barium titanate-lead zirconate titanate solid solutions by a modified mixed-oxide synthetic route, Curr. Appl. Phys. 4 (2–4) (2004) 182–185.
- [6] W. Chaisan, R. Yimnirun, S. Ananta, D.P. Cann, Dielectric properties of solid solutions in the lead zirconate titanate-barium titanate system prepared by a modified mixed-oxide method, Mater. Lett. 59 (2005) 3732–3737.
- [7] JCPDS-ICDD card no. 37-1484, International Centre for Diffraction Data, Newtown Square, PA, 2002.
- [8] S. Fushimi, T. Ikeda, Phase equilibrium in the system PbO-TiO₂-ZrO₂, J. Am. Ceram. Soc. 50 (1967) 129–132.
- [9] Z. Brankovic, G. Brankovic, J.A. Varela, PZT ceramics obtained from mechanochemically synthesized powders, J. Mater. Sci. 14 (2003) 37–41
- [10] F. Xia, X. Yao, Piezoelectric and dielectric properties of PZN-BT-PZT solid solutions, J. Mater. Sci. 34 (1999) 3341–3343.
- [11] N. Vittayakorn, G. Rujijanagul, T. Tunkasiri, X. Tan, D.P. Cann, Influence of processing conditions on the phase transition and ferroelectric properties of Pb(Zn_{1/3}Nb_{2/3})O₃-Pb(Zr_{1/2}Ti_{1/2})O₃ ceramics, Mater. Sci. Eng. B 108 (2004) 258–265.
- [12] V.L. Balkevich, C.M. Flidlider, Hot-pressing of some piezoelectric ceramics in the PZT system, Ceramurgia Inter. 2 (1976) 81–87.
- [13] M. Ausloos, Dielectric response of composite materials, J. Phys. C: Solid State Phys. 18 (1985) L1163–L1167.
- [14] S.R. Panteny, C.R. Bowen, R. Stevens, Piezoelectric Particulate Reinforced Nanocomposites, The Alden Group, Oxford, 2000.





CERAMICS INTERNATIONAL

www.elsevier.com/locate/ceramint

Ceramics International 35 (2009) 173-176

Effect of vibro-milling time on phase formation and particle size of barium titanate nanopowders

W. Chaisan *, R. Yimnirun, S. Ananta

Department of Physics, Faculty of Science, Chiang Mai University, Chiang Mai 50200, Thailand
Accepted 1 October 2007
Available online 26 February 2008

Abstract

Barium titanate (BT) nanopowder was synthesized by a solid state reaction via a rapid vibro-milling technique. The effect of milling time on phase formation and particle size of BT powder was investigated. Powder samples were characterized using XRD (X-ray diffraction) and SEM techniques. It was found that the resulting BT powders have a range of particle size depending on milling times. Production of a single-phase BT nanopowder can be successfully achieved by employing a combination of 30 h milling time and calcination conditions of 1200 °C for 2 h. © 2008 Elsevier Ltd and Techna Group S.r.l. All rights reserved.

Keywords: A. Milling; Powders: solid state reaction; D. BaTiO₃

1. Introduction

Barium titanate (BaTiO₃ or BT), which exhibits a perovskite structure and a Curie temperature $\sim \! 120~^{\circ}\text{C}$, is a classical ferroelectric material that has been extensively exploited both for academic and technological utilizations over the past decades [1,2]. Owing to its high dielectric constant, large mechanical-quality factor, large pyroelectric coefficient, nontoxic handling and low cost of manufacturing, compared to several lead-based perovskite ferroelectrics, BT-based ceramics have been a strong candidates for several electronic applications, including ultrasonic transducers, multilayer capacitors, pyroelectric detectors, semiconductors with positive temperature coefficient of resistance (PTCR) and electro-optic devices [3,4]. To fabricate them, a fine powder of perovskite phase with a minimal degree of particle agglomeration is needed as the starting material to achieve a dense and uniform microstructure at a given sintering temperature. In order to improve the sintering behavior of ceramics, a crucial focus of powder synthesis in recent years has been the formation of uniformsized, single morphology particulates ranging in size from nanometer to micrometers.

The development of a method to produce nanopowders of precise stoichiometry and desired properties is complex, depending on a number of variables such as nature and purity of starting materials, processing history, temperature, etc. To obtain nanosized BT powders, many investigations have focused on several chemistry-based preparation routes, such as sol-gel [5], sol-precipitation [6], hydrothermal reaction [7], besides the more conventional solid state reaction of mixed oxides [8]. All these techniques are aimed at reducing the particle size and temperature of preparation of the compound even though they are more involved and complicated in approach than the solid state reaction. The advantage of using mechanical milling for preparation of nanosized powders lies in its ability to produce mass quantities of powders in the solid state using simple equipment and low cost starting precursors [9,10]. The ball-milling technique is a very popular solid state reaction because of easy and low cost technique, however the size of particle from this technique is still large (micrometer). Thus, the potentiality of vibro-milling technique will be then focused in order to achieve the nanosized powder. Although some research has been done in the preparation of BT nanopowders via a vibro-milling technique [11], to our knowledge a systematic study regarding the influence of milling time on the preparation of BT nanopowders has not yet been reported. Therefore, in this work, the effect of milling time on phase formation, and particle size of BT nanopowders was investigated in this connection. The potential of the vibro-

^{*} Corresponding author. Tel.: +66 53 943376; fax: +66 53 943445. E-mail address: wanwilai_chaisan@yahoo.com (W. Chaisan).

milling technique as a simple and low-cost method to obtain usable quantities of single-phase BT powders at low temperature and with nanosized particles was also examined.

2. Experimental procedure

Commercially available powders of BaCO3 and TiO2 (anatase form), (Fluka, >99% purity) were used as starting materials. BaTiO₃ powder was synthesized by the solid state reaction of these raw materials. A vibratory laboratory mill (McCrone Micronizing Mill) powered by a 1/30 HP motor was employed for preparing the stoichiometric BaTiO₃ powder [9]. The mixed powder was vibro-milled for 0.5 h with corundum media in isopropyl alcohol (IPA). Drying was carried out for 2 h at 120 °C. Various calcination temperatures ranging from 700 to 1400 °C were selected to investigate the phase development of BT. Moreover, in order to investigate the effect of milling time on phase formation and particle size, the milling times were then ranged from 0.5 to 30 h. All powders were examined by room temperature X-ray diffraction (XRD; Siemens-D500 diffractometer) using Ni-filtered Cu Kα radiation, to identified the phase formed and the optimum firing temperature for the production of single-phase BT powders under various milling conditions. The crystallite size and tetragonality factor (c/a)were also estimated from these XRD patterns [12]. The morphologies of the powders observed by scanning electron microscopy (JEOL JSM-840 A SEM).

3. Results and discussion

From the TG-DTA data in previous work [13], the range of calcination temperatures between 700 and 1400 °C were designed for BT powder to investigate the phase formation. To study the phase development with increasing calcination temperature in BT powder prepared from vibro-milling technique for 0.5 h, it was calcined for 2 h in air at various temperatures, up to 1400 °C, followed by phase analysis using XRD. As shown in Fig. 1, for the uncalcined powder, only X-ray peaks of precursors, BaCO₃ (\bullet) and TiO₂ (\bullet), which could be matched with JCPDS file numbers 5-0378 [14] and 21-1272 [15], respectively, are presented, indicating that no reaction had yet been triggered during the milling process. In this work, it is seen that the desired perovskite BaTiO₃ (\bigtriangledown) was already observed in the powder calcined at 700 °C, accompanying with unreacted BaCO₃ and TiO₂ precursors as

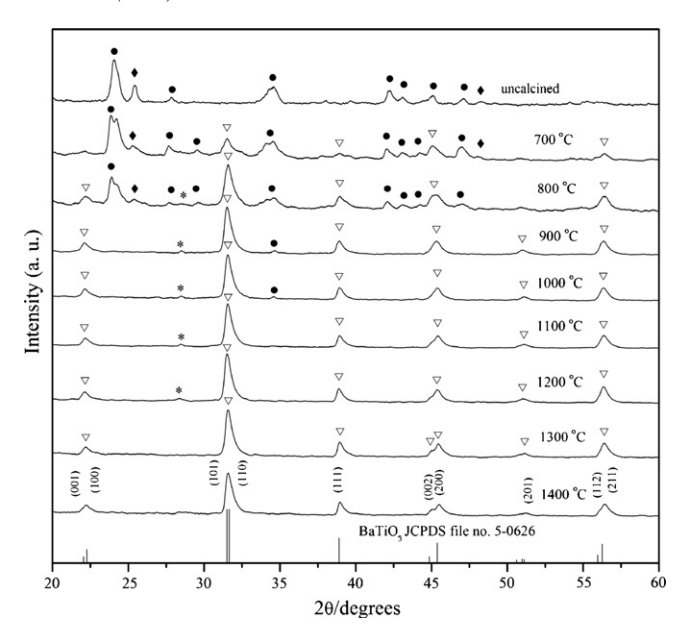


Fig. 1. XRD patterns of BT powders calcined at various temperatures for 2 h with heating/cooling rates of 10 °C/min (\bullet = BaCO₃, \diamond = TiO₂, ∇ = BaTiO₃ and * = Ba₂TiO₄).

separated phases, in good agreement with literature [16,17]. Moreover, the unknown phase (\star) started to occur at $2\theta \sim 28.5^{\circ}$, consistent with earlier work of Simon-Seveyrat et al. [18]. According to the literature [19,20], the reaction sequence of the phase formation in the BT mixture can be described as follow.

$$2BaCO_3 + TiO_2 \rightarrow Ba_2TiO_4 + 2CO_2 \tag{1}$$

$$Ba_2TiO_4 + TiO_2 \rightarrow 2BaTiO_3$$
 (2)

It was believed that this unknown phase corresponds to Ba_2TiO_4 , which could be matched with JCPDS file numbers 72-0135 [21], always found in conventional mixed oxide processing [16,22]. As the temperature increased to $1000\,^{\circ}$ C, the intensity of the $BaTiO_3$ peaks was further enhanced. The starting materials completely disappeared after calcination at $1100\,^{\circ}$ C, however, the unwanted Ba_2TiO_4 phase still be detected. Upon calcination at $1300\,^{\circ}$ C, an essentially monophasic of $BaTiO_3$ phase was obtained. This observation agrees well with other workers [23,24]. This BT phase was indexable according to a tetragonal perovskite-type structure with lattice parameters $a=3.994\,^{\circ}$ A and $c=4.038\,^{\circ}$ A, space group P4mm (no. 99), consistent with JCPDS file number 5-0626 [25].

Table 1

Effect of milling time on the optimum calcination temperature and the variation of particle size of BT powders measured by different techniques

Milling time (h)	Perovskite phase (%)	Calcination temperature (°C)	XRD		SEM	
			A (nm)	cla	D (nm)	P (nm)
0.5	100	1300	38.32	1.0090	610	250-1400
10	100	1250	32.09	1.0059	260	100-500
15	100	1250	32.38	1.0036	490	100-1000
20	100	1250	31.95	1.0058	590	250-700
25	100	1200	31.60	1.0065	390	250-700
30	100	1200	31.56	1.0056	250	100-400

A = crystallite size, c/a = tetragonality factor, D = average particle size, P = particle size range.

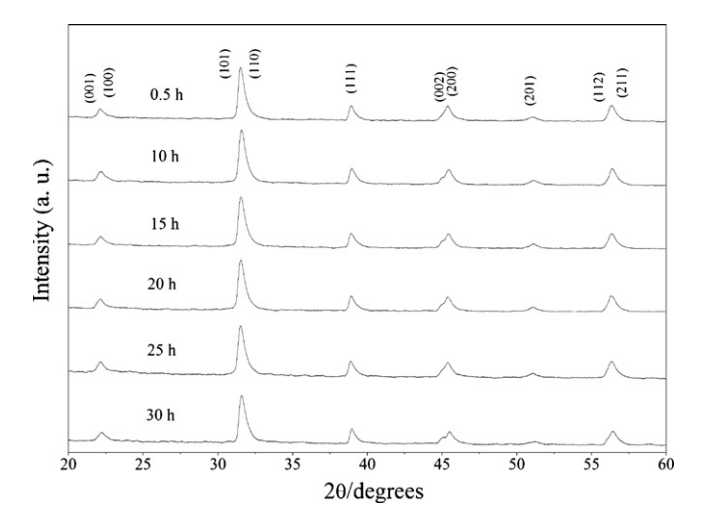


Fig. 2. XRD patterns of BT powders milled at different times.

Having established the optimum calcination temperature of BT powder vibro-milled for 0.5 h, an attempt was also made to calcine the BT powder under various milling times. The optimum calcination temperature of each powder was reported in Table 1 and the XRD patterns of all BT powders are shown in Fig. 2. It has been observed that with increasing milling time, all diffraction lines broaden, e.g., (0 0 2) and (2 0 0) peaks, an indication of a continuous decrease in particle size and of the introduction of lattice strain. These values indicate that the prolonged milling treatment affects the particle size and evolution of crystallinity of the phase formed. For BT powders, the longer the milling time, the lower the required (optimum)

firing temperature. Additionally, the crystallite size and tetragonality factor (*c/a*) were estimated from these XRD patterns as also given in Table 1. The calculated crystalline size value was also found to decrease with increasing milling time. Though, the relative intensities of the Bragg peaks and the calculated tetragonality factor (*c/a*) for the powders exhibit independent of milling time, it is well documented that, as Scherer's analysis provides only a measurement of the extension of the coherently diffracting domains, the crystallite sizes determined by this method can be significantly under estimation [26]. In addition to strain, factors such as dislocations, stacking faults, heterogeneities in composition and instrumental broadening can attribute to peak broadening, making it almost impossible to extract a reliable particle size solely from XRD [27].

In this connection, SEM was also employed for particle size measurement (Table 1). The morphological evolution of the powders as a function of milling time was also revealed, as illustrated in the SEM micrographs (Fig. 3). At first sight, the morphological characteristic of BT powders with various milling times is similar for all cases. In general, the particles are agglomerated and basically irregular shape, with a substantial variation in particle sizes. The powders consist of primary particles with nanometers in size. Increasing milling time over the range 0.5–30 h, the powders exhibit spatial fluctuation in their particle sizes. The extent of the fluctuation depends on the milling time as well as on the calcination temperature applied. In this study, it is seen that the optimum milling time for the production of the smallest nanosized BT powder with low firing temperature was found to be at 30 h. The finding of this

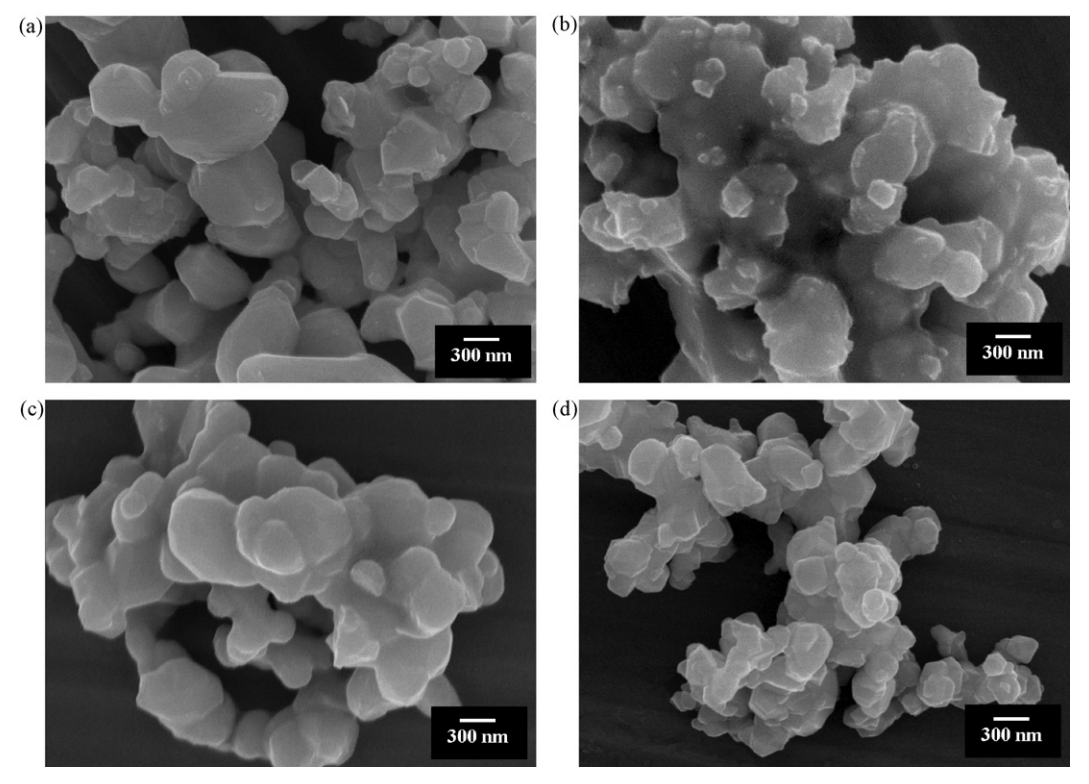


Fig. 3. SEM micrographs of BT powders after milling times of (a) 0.5, (b) 15, (c) 25 and (d) 30 h (calcined at their optimized conditions).

investigation indicates a strong relationship between the vibromilling process and the yield of BT nanopowders.

4. Conclusions

The synthesis of perovskite BT nanopowder by a solid state reaction and the influence of milling time on its formation were studied. It was established that the milling time influences not only the development of the solid state reaction of BT phase but also particle size and morphology. It was shown that the increase of vibro-milling time significantly decreases the calcination temperature and particle size. A single phase of BT nanopowder can be successfully produced by employing a combination of 30 h milling time and calcination condition of 1200 °C for 2 h.

Acknowledgements

I would like to thank the Thailand Research Fund (TRF), Commission on Higher Education (CHE) and the Faculty of Science, Chiang Mai University for all financial support.

- A.J. Moulson, J.M. Herbert, Electroceramics: Materials, Properties, Applications, John Wiley & Sons Ltd., Chichester, 2003.
- [2] G.H. Haertling, Ferroelectric ceramics: history and technology, J. Am. Ceram. Soc. 82 (4) (1999) 797–818.
- [3] K. Uchino, Piezoelectrics and Ultrasonic Applications, Kluwer, Deventer, 1998.
- [4] Y. Xu, Ferroelectric Materials and their Applications, Elsevier Science Publishers B.V., 1991.
- [5] S. Tangwiwat, S. Milne, Barium titanate sols prepared by a diol-based solgel route, J. Non-Cryst. Solids 351 (12/13) (2005) 976–980.
- [6] W. Luan, L. Gao, J. Guo, Study on drying stage of nanoscale powder preparation, NanoStruct. Mater. 10 (7) (1998) 1119–1125.
- [7] S. Kwon, D. Yoon, Effects of heat treatment and particle size on the tetragonality of nano-sized barium titanate powder, Ceram. Int. 33 (7) (2007) 1357–1362.
- [8] J. Chen, Z. Shen, F. Liu, X. Liu, J. Yun, Preparation and properties of barium titanate nanopowder by conventional and high-gravity reactive precipitation methods, Scripta Mater. 49 (2003) 509–514.
- [9] R. Wongmaneerung, R. Yimnirun, S. Ananta, Effect of vibro-milling time on phase formation and particle size of lead titanate nanopowders, Mater. Lett. 60 (12) (2006) 1447–1452.

- [10] R. Wongmaneerung, T. Sarakonsri, R. Yimnirun, S. Ananta, Effects of milling method and calcination condition on phase and morphology characteristics of Mg₄Nb₂O₉ powders, Mat. Sci. Eng. B 130 (2006) 246–253.
- [11] B.D. Stojanovic, C. Jovalekic, V. Vukotic, A.Z. Simoes, J.A. Varela, Ferroelectric properties of mechanically synthesized nanosized barium titanate, Ferroelectrics 319 (2005) 65–73.
- [12] C. Suryanarayana, M.G. Norton, X-Ray Diffraction: A Practical Approach, Plenum Press, New York, 1998.
- [13] W. Chaisan, Preparation and Characterization of Ceramic Nanocomposite in the PZT-BT and TiO₂-SnO₂ Systems, Ph.D. Thesis, Chiang Mai University, Chiang Mai, Thailand, 2006.
- [14] JCPDS-ICDD card no. 5-0378, International Centre for Diffraction Data, Newtown Square, PA, 2002.
- [15] JCPDS-ICDD card no. 21-1272, International Centre for Diffraction Data, Newtown Square, PA, 2002.
- [16] V. Berbenni, A. Marini, G. Bruni, Effect of mechanical milling on solid state formation of BaTiO₃ from BaCO₃-TiO₂ (rutile) mixtures, Thermochim. acta 374 (2) (2001) 151–158.
- [17] E. Brzozowski, M.S. Castro, Synthesis of barium titanate improved by modifications in the kinetics of the solid state reaction, J. Eur. Ceram. Soc. 20 (2000) 2347–2351.
- [18] L. Simon-Seveyrat, A. Hajjaji, Y. Emziane, B. Guiffard, D. Guyomar, Reinvestigation of Synthesis of BaTiO₃ by conventional solid-state reaction and oxalate coprecipitation route for piezoelectric applications, Ceram. Int. 33 (1) (2007) 35–40.
- [19] A. Beauger, J.C. Mutin, J.C. Niepce, Synthesis reaction of metatitanate BaTiO₃. Part 2: study of solid-solid reaction interfaces, J. Mat. Sci. 18 (1983) 3543–3550.
- [20] L.B. Kong, J. Ma, H. Huang, R.F. Zhang, W.X. Que, Barium titanate derived from mechanochemically activated powders, J. Alloys Compd. 337 (2002) 226–230.
- [21] JCPDS-ICDD card no. 72-0135, International Centre for Diffraction Data, Newtown Square, PA, 2002.
- [22] J.K. Lee, K.S. Hong, J.W. Jang, Roles of Ba/Ti ratios in the dielectric properties of BaTiO₃ ceramics, J. Am. Ceram. Soc. 84 (9) (2001) 2001– 2006
- [23] W. Chaisan, S. Ananta, T. Tunkasiri, Synthesis of barium titanate-lead zirconate titanate solid solutions by a modified mixed-oxide synthetic route, Cur. Appl. Phys. 4 (2–4) (2004) 182–185.
- [24] W. Chaisan, R. Yimnirun, S. Ananta, D.P. Cann, Dielectric properties of solid solutions in the lead zirconate titanate-barium titanate system prepared by a modified mixed-oxide method, Mater. Lett. 59 (2005) 3732–3737.
- [25] JCPDS-ICDD card no. 5-0626, International Centre for Diffraction Data, Newtown, PA, 2002.
- [26] C. Suryanarayana, Mechanical alloying and milling, Prog. Mater. Sci. 46 (2001) 1–184.
- [27] H. Klug, L.E. Alexander, X-ray Diffraction Procedures for Polycrystalline and Amorphous Materials, Wiley, New York, 1974.

Composition, Structure and Properties of PZT-BT Ceramics Prepared by Two-stage Sintering

Wanwilai C. Vittayakorn^{1*}, Rattikorn Yimnirun² and Supon Ananta³

¹Department of Physics, Faculty of Science, Chiang Mai University, Chiang Mai THAILAND

Keywords: sintering, PZT, BT.

ABSTRACT

Ceramic solid solutions within the system (1-x)PZT-xBT, where x = 0.1, 0.2, 0.3, 0.4 and 0.5, were prepared by conventional mixed-oxide method combined with a two-stage sintering procedure. A sintering time of 2 h at 1000 °C followed by a second step in the temperature range of 1000-1200 °C for 2 h was employed to all samples and compared to the one-step sintering process. Phase formation, densification and microstructure of all ceramics were examined via X-ray diffraction (XRD), Archimedes method and scanning electron microscope (SEM). The results lead to the conclusion that the pure perovskite phase and high densification of (1-x)PZT-xBT ceramics with fine grain can be successfully achieved under suitable two-stage sintering conditions.

INTRODUCTION

Lead-based ferroelectric ceramics are widely used in smart electronic devices such as actuators and micro-positioners because of their favorable characteristics [1]. Both PZT and BT are among the most common ferroelectric ceramics and have been studied extensively since the late 1940s [2]. These two ceramics have distinct characteristics that make each ceramic suitable for different The PZT ceramic has great piezoelectric properties which can be applied in transducer and actuator applications. Moreover, it has a high T_C of 390 °C allowed devices to be operated at high temperatures. BT ceramic is a classical ferroelectric material which exhibits a high dielectric constant, large mechanical-quality factor and large pyroelectric coefficient. mixing PZT with BT is expected that excellent properties with preparation ease can be obtained from ceramics in the PZT-BT system. Furthermore, the electrical properties of ferroelectric ceramics depend strongly on microstructure as well as chemical compositions. It was reported earlier that the high value of dielectric constant can be revealed if polycrystalline ferroelectric ceramics of fine grain size is achieved. Thus, a fine grain is essential to achieve optimum dielectric properties. It is well known that the microstructure of most ferroelectric ceramics can be normally controlled by two approaches. Utilizing additives to prohibit the grain growth is one approach [3]. Another approach uses novel processing technique to modify the microstructure. Numerous studies on the sintering of ferroelectric ceramics have been reported in the literature [4]. Recently, a two-stage sintering method has been proposed by Chen and Wang to achieve the densification of ceramic bodies without significant grain growth [5]. Since the two-stage sintering process is a low-cost technique and simple ceramic fabrication to obtain highly dense ceramics with pure phase, therefore, in this work a two-stage sintering method has been adopted to produce the The influence of two-stage sintering condition on phase fine grain (1-x)PZT-xBT ceramic. formation, densification and microstructure of all ceramics is investigated.

²Department of Physics, Faculty of Science, Chiang Mai University, Chiang Mai THAILAND

³Department of Physics, Faculty of Science, Chiang Mai University, Chiang Mai THAILAND

METHOD

(1-x)Pb(Zr_{0.52}Ti_{0.48})O₃–xBaTiO₃ or (1-x)PZT–xBT powders, where x = 0.1, 0.2, 0.3, 0.4 and 0.5, were prepared by a conventional mixed-oxide method. Commercially powders of PbO, ZrO₂, BaCO₃ and TiO₂ were used as starting materials. PZT and BT powders were first form in order to avoid unwanted pyrochlore phases. The (1-x)PZT–xBT powders were then formulated from the PZT and BT precursors by employing the similar mixed-oxide procedure. After ball-milling for 24 h in ethanol, the slurry was dried at 120 °C and calcined in a closed alumina crucible with the optimum calcination conditions for each composition. The calcined powders were then pressed to pellets with 15.0 mm of diameter and 1.0 mm of thickness using an uniaxial die press at 50 MPa. In the so-called two-stage sintering process, the first sintering temperature was assigned for 1000 °C and variation of the second sintering temperature between 1000 °C and 1200 °C was carried out. For comparison, normal sintering process was also carried out at the firing temperature between 1150 and 1350 °C for 2 h. Phase formation, densification and microstructure development of all final sintered products were determined by using the X-ray diffractometer (XRD), Archimedes principle and scanning electron microscopy (SEM), respectively.

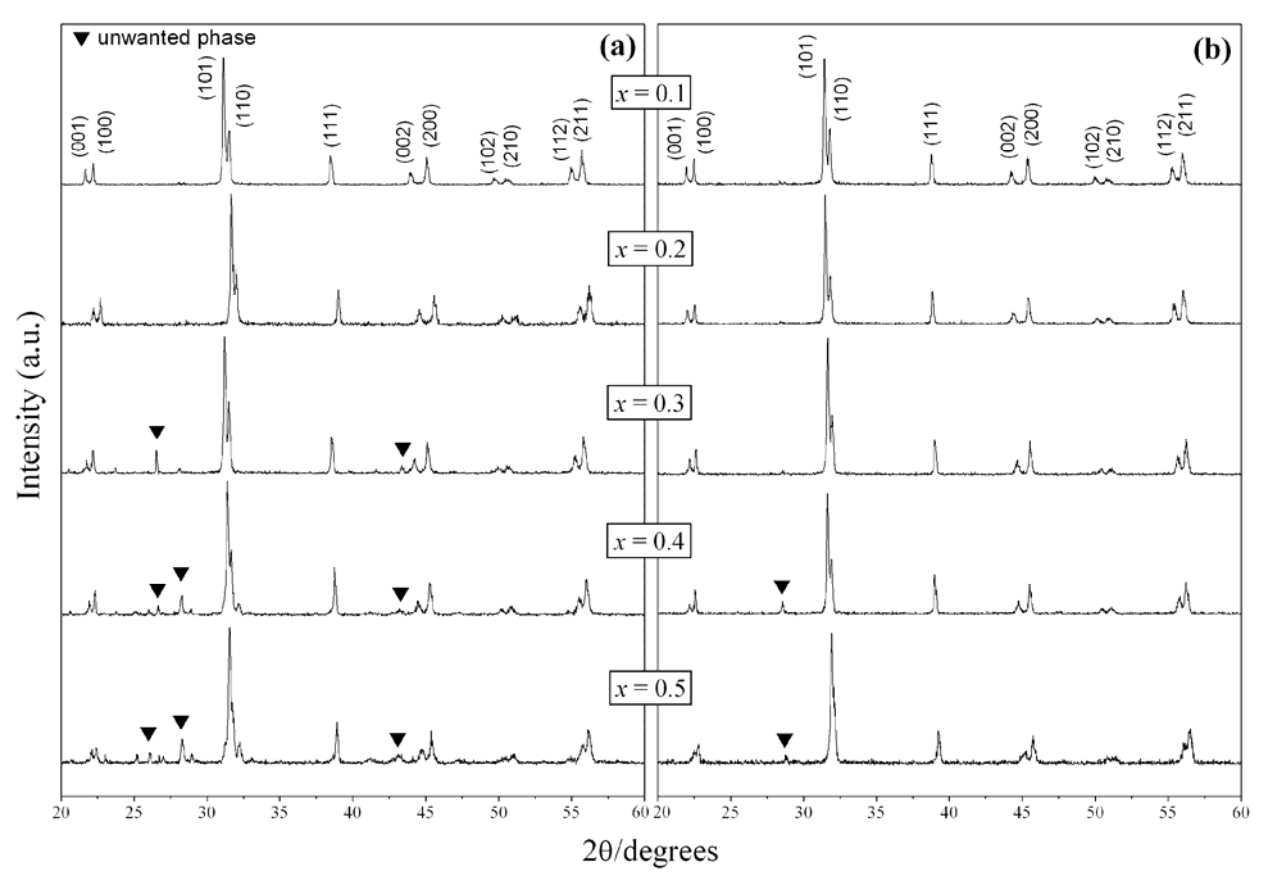


Fig. 1. XRD patterns of (1-x)PZT-xBT ceramics prepared by (a) two-stage sintering compared with (b) normal sintering.

RESULTS AND DISCUSSION

The XRD patterns of two-stage sintered (1-x)PZT-xBT ceramics at various compositions compared with normal sintered ceramic are illustrated in Fig. 1. The XRD graphs for both sintering techniques show slightly different peaks. From Fig. 1(a), it can be indicated that the pure perovskite phase of two-stage sintered ceramics was found in the compositions of x = 0.1 and 0.2, whereas the unwanted phase can be detected with increasing of x. Likewise, the same situation

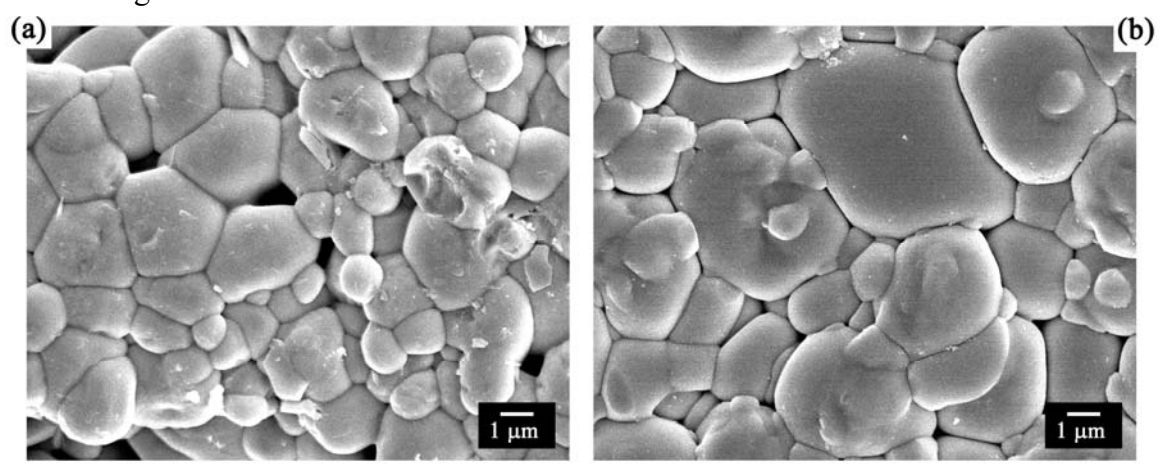
was also found in normal sintered ceramics but less. The compositions of x = 0.1, 0.2 and 0.3 show XRD peaks of pure perovskite phase (Fig. 1(b)), while the graphs of 0.6PZT-0.4BT and 0.5PZT-0.5BT ceramics indicate perovskite phase with traces of unwanted peaks. With carefully investigation, it is believed that this unwanted phase (∇) which occur in both sintering techniques is ZrO₂ matched with JCPDS file no. 37-1484. Compositional fluctuations due to the evaporation of lead oxide within surface regions are believed to be responsible for the occurrence of free ZrO₂ phase in the sintered (1 - x)PZT-xBT ceramics.

Table 1 Characterizations of sintered (1-x)PZT-xBT ceramics.

	Two-stage sintering			Normal sintering			
x (BT content)	Sintering temperature (°C)	Relative density (%)	Average grain size (µm)	Sintering temperature (°C)	Relative density (%)	Average grain size (μm)	
0.5	1150	71.90	3.47	1250	84.92	3.55	
0.4	1200	77.36	2.55	1250	81.82	3.33	
0.3	1150	78.19	2.75	1250	85.24	3.34	
0.2	1200	81.47	2.56	1300	99.29	3.79	
0.1	1200	78.50	2.82	1300	94.19	4.03	

The effect of sintering techniques on the densification and microstructure for (1-x)PZT-xBT ceramics are listed in Table 1. Generally, it is evident that the relative densities obtained by two-stage sintering are slightly lower than that of ceramics sintered by conventional in all compositions. Normal sintered ceramics reached a maximum density of ~ 99% at 1300 °C for single phase 0.8PZT-0.2BT. On the other hand, two-stage sintered samples exhibit reduced densification, and a temperature of 1200 °C was required to reach a densification level of ~81% for the same composition. However, even the densification of two-stage sintered ceramics decreases but the required sintering temperature for each composition is also significantly reduced. Moreover, from Table 1, it is seen that the average grain size of the two-stage sintered ceramics is much smaller than that of normal sintered ceramics for all compositions. microstructures of PZT-BT ceramic (x = 0.2) which exhibit the highest density sintered with different schemes were revealed by SEM and shown in Fig. 2. SEM micrographs show that for the first approximation both ceramics exhibit good densification and homogenous grain size. However, it can be noticed the microstructure of the two-stage sintered ceramics (Fig. 2a) is slightly different from that of the normal sintered samples (Fig. 2b). Grain size of normal sintered ceramic varies greatly from 0.5 to 10 µm whereas the two-stage sintered ceramic contains smaller average grain size (~ 2.5 µm) and some degree of porosity is clearly seen. In addition, other compositions also show the same trend of grain size compared between two different sintering schemes. For comparison, even though exact mechanism of the microstructure observed here is not well established, but it should be noted that the various features of microstructure in PZT-BT ceramics are dependent on the grain growth rate in the different planes [6]. However, the sintering process and growth environment also play an important role in the formation [7]. More importantly, it can be assumed that the two-stage sintering process could suppress the grain growth mechanism efficiently whereas the relative density of both normal- and two-stage sintered ceramics is in high value. This can be explained that the feasibility of densification without grain growth, which is believed to occur in two-stage sintered ceramic, relies on the suppression of grain boundary migration while keeping grain boundary diffusion active. The kinetic and the driving force for grain growth behavior in the second-step sintering were previously discussed by Chen and Wang [5]. Their work suggested that the suppression of the final stage grain growth was achieved by exploiting the difference in kinetics between grain-boundary diffusion and grain-boundary migration.

Fig. 2. SEM micrographs of sintered 0.8PZT-0.2BT ceramics: (a) two-stage sintering and (b) normal sintering.



CONCLUSION

Even though the simple mixed-oxide method employing a conventional ball-milling was used, this work demonstrated that it was possible to obtain smaller grain size ferroelectric (1-x)PZT-xBT ceramics with high densification by the two-stage sintering technique. It has been shown that, under suitable condition, two-stage sintering can effectively suppress the grain growth in this system leading to small-grained microstructure.

ACKNOWLEDGEMENTS

This work was supported by the Thailand Research Fund (TRF), Commission on Higher Education (CHE) and Faculty of Science of Chiang Mai University.

REFERENCES

- [1] K. Uchino, "Ferroelectric Devices", (Marcel Dekker, New York, 2000), pp 1-308.
- [2] G. H. Haertling, J. Am. Ceram. Soc., 82 (1999), p. 797.
- [3] A. Yamaji, Y. Enomoto, K. Kinoshita, T. Murakami, J. Am. Ceram. Soc., 60 (1977), p. 97.
- [4] H. T. Kim, Y. H. Han YH, Ceram. Int., 30 (2004), p. 1719.
- [5] I. W. Chen, X. H. Wang, Nature, 404 (2000) p. 168.
- [6] M. H. Lin, J. F. Chou, H. Y. Lu, J. Eur. Ceram. Soc., 20 (2000), p. 517.
- [7] R. M. German, "Sintering Theory and Practice", (Wiley, New York, 1996), pp. 1-550.

e-mail: wanwilai chaisan@yahoo.com

Fax: +66-53-94-3445